FINAL REPORT, NSG-6014

1 JANUARY 1976 to 31 DECEMBER 1979

# ACTIVE EXPERIMENTS USING ROCKET-BORNE SHAPED CHARGE BARIUM RELEASES

Report prepared by Eugene M. Wescott

Geophysical Institute
University of Alaska
Fairbanks, Alaska 99701

(NASA-CR-162581) ACTIVE EXPERIMENTS USING ROCKET-BORNE SHAPED CHARGE BARIUM RELEASES (Alaska Univ., Fairbanks.) 84 p
HC A05/MF A01 CSCL 04A

N80-15708

Unclas
G3/46 46904

January 15, 1980

NASA Grant NSG-6014
Principal Investigators:
T. N. Davis and E. M. Wescott

Participating Scientists:
H. C. Stenbaek-Nielsen
T. J. Hallinan

## Introduction

Prior to the period covered by contract NSG-6014, NASA had supported the Geophysical Institute in a series of rocket-borne active experiments which were carried out as a cooperative program with Los Alamos Scientific Laboratory and Sandia Corporation. We achieved many noteworthy scientific discoveries (Wescott et al., 1972, 1974, 1975a, 1975b, 1976a, 1976b, 1978; Jeffries et al., 1975; Swift et al., 1976; Winningham et al., 1977) using our low-light-level observational techniques and geophysical experience coupled with the resources of LASL for explosives technology and Sandia for payload and rocket support. In 1976, due to various circumstances, further cooperative programs along these lines became impossible, and we proposed a scaled down yet viable program of active experiments with the assistance of Wallops Flight Center.

The shaped charge we had developed with LASL was intended for a Sandhawk-Tomahawk or larger rocket, and required an exotic explosive and very expensive casting and machining. The payload was elegant, containing a three-axis attitude control system, and required a Sandhawk-Tomahawk or Black Brant IV rocket to attain sufficient altitude. We were forced by funding limitations to develop a less expensive system to carry out fruitful active experiments aimed at solving outstanding problems of solar-terrestrial magnetospheric physics.

Initially we were told we could plan on one Nike-Malemute rocket, equal to or superior to those we had used in the past. Upon investigation we found that a very short payload (102 cm) of about 28 kg on a Nike-Tomahawk could, in theory, achieve the altitude required for barium shaped charge experiments. We received permission to proceed with two

Nike-Tomahawk flights in 1977. Over the last four years we have developed a reliable payload system with Wallops Flight Center, have developed scaled down state-of-the-art shaped charges, and have carried out a series of successful experiments from Poker Flat Research Range.

We also continued work on improving our low-light-level TV observing capabilities and participated in several experiments with the Max-Planck-Institute group.

The Max-Planck-Institute Project Porcupine

As part of the first year's effort on the project, we mounted an image orthicon TV imaging system in a NASA Learjet based at Ames Research Center, and operated the system in March 1976 in support of Project Porcupine. The observations were conducted in aircraft flights out of Athens, Greece. Although the operation itself was without flaw, no useful data were obtained due to failure of the rockets used to launch the first Porcupine payload.

In March 1977 the second Porcupine attempt was successful and we obtained excellent data from the Learjet out of Athens. A short paper on the experiment has been published (Rieger et al., 1979).

Subsequently we have also participated in two more successful Porcupine experiments, improving our observational equipment and techniques. We have also used the NASA Learjet to observe our own barium plasma injection experiments 12.1003 UE and 12.1004 UE in March 1979.

H. C. Stenbaek-Nielsen spent part of his sabbatical leave in 1978-79 at the Max-Planck-Institute.

Rocket Experiments 18.1011 UE and 18.1012 UE

Initially we had proposed to test a new concept of particle acceleration on a payload to be flown on a Nike-Malemute rocket. Early in the project we discovered that it was feasible to lift a short, light payload on a Nike-Tomahawk to near the minimum altitude required. This altitude of 450 km is where high-speed barium ions can be injected upwards without excessive loss through collisions with the ambient atmosphere. Two nearly-identical payloads were designed and fabricated, with a major portion of the structural design and fabrication being performed by personnel of Wallops Flight Center. Each payload incorporated an array of four shaped charge assemblies three inches in diameter and containing 50 gm barium metal liners. The shaped charges were detonated simultaneously using TLX cord from a common detonator.

One payload incorporated an accelerating stage ahead of each shaped charge. This consisted of an electrostatic grid array attached to a cylindrical piezoelectric ceramic. When rapidly compressed the cylinder produces a very high voltage. The compression of the cylinder was accomplished by a cylindrical shell of explosive around its circumference that was detonated by the advancing shock front from the main charge. The timing of the piezoelectric voltage pulse was designed to provide ionization and acceleration of the high-velocity barium vapor for about 10 microseconds before the electrostatic grid was destroyed.

Besides a savings on weight and cost for four small shaped charges and piezoelectric cylinders rather than one large one, Eichelburger and Pugh (1952) and Eichelberger (1955) showed by theory and experiments that the tip of the high-velocity jet formed by a shaped charge detonation comes from the liner element originally close to the apex of the liner. Slower elements of the jet came from elements of the liner further from

the apex. Consequently, we thought it possible that four truncated charges might produce a higher proportion of high-velocity (near 13 km/sec) gas in the jet as compared to a larger single shaped charge.

Nike-Tomahawk rocket 18.1011 was launched successfully during evening twilight from Poker Flat on February 7, 1977. The accelerated stage shaped charges were detonated at 444.6 km altitude during quiet magnetic conditions. The second Nike-Tomahawk, 18.1012 UE without the accelerator stages was launched successfully under similar conditions on February 11, 1977. Detonation occurred at 447.2 km altitude.

Up to that time, these were the highest altitudes achieved by Nike-Tomahawk rockets, demonstrating the feasibility of their use for barium plasma injection experiments. Mechanically both payloads, which weighed 29.1 kg, performed flawlessly.

Both payloads produced usable plasma jets; however, the overall free barium observed in the detonation incorporating the piezoelectric acceleration stage was less than without the stage, indicating that the stage interferred with the vaporization process.

The velocity distribution of ions in the two was also markedly different: There was a "hole" in the number density vs velocity distribution for 18.1011 between 5 and 7 km/sec, which was not apparent in the standard payload. The slit photometer which was to detect and measure the velocity of any accelerated ions was not pointed in the proper place due to deviation of the rocket trajectory from nominal, consequently if some ions were accelerated to higher velocities they could not be detected. There is a possibility that the missing ions (5 - 7 km/sec) were accelerated to high velocity but were never seen. It is also possible that several

things may have gone wrong in the accelerator scheme, such as: barium vapor or explosive products shorting out the rear end of the piezoelectric cylinder; excess pressure transferred to the cylinder; the rarefaction wave followed the compression wave too closely, cancelling out the voltage; the collapsing cylinder causing a reflected shock wave which interferred with the jet development.

In any case, the accelerator stage was not beneficial. The results also showed that except for cost, there was no advantage to clustering small truncated charges, as a single larger shaped charge of optimum design would produce more barium ions. Calculations showed that on a Nike-Tomahawk rocket a 15.24 cm diameter shaped charge weighing 11.8 kg could be flown with the same proven payload hardware and performance as 18.1011 and 18.1012.

The quiet magnetic and auroral conditions of these two launches did not produce any new scientific results on ionospheric or magnetospheric electric fields.

18.1018 UE and 18.1019 UE

Theoretical studies to improve the performance of the plasma jet continued in 1977 with the aims of: 1) producing ions more efficiently for given weight and space, 2) reduce the ion velocity dispersion closer to a monoenergetic beam, 3) increase the velocity and, 4) ionize the barium as it exits the shaped charge.

The use of piezoelectric crystals to provide an ionizing and accelerating voltage pulse was shelved for several reasons: 1) extreme difficulties in scaling up to significant energy release within rocket and payload

weight limitations, 2) a reduction in our funding which made a proposed ground testing and development program not feasible, and 3) estimations that other schemes looked more promising.

After an exhaustive search for an American supplier, we were unable to find any company who would manufacture the barium metal cones needed for new experiments. We had sources for the explosive shaped charges, however.

Dr. Gerhard Haerendel of the Max-Planck-Institute while on a visit to the Geophysical Institute kindly offered to assist in procuring the barium cones from his facility in Germany. As it became evident that there would be a problem in matching the barium cones to our shaped charges without shipping them to Germany to be joined, he offered to also fabricate the shaped charges. We decided to use a different design concept than that which we had optimized with the LASL-UA complex cone model, which is difficult and expensive to machine. The Max-Planck-Institute group had flown several successful shaped charges utilizing a wave shaper and a tapered conical liner with good results. The peak velocity was almost comparable to the LASL model with improved velocity distribution and dispersion.

MPI contracted an outside consultant, Professor Thomanek of Messerschmitt Boelkov-B, to optimize the shaped charge and liner given our size and weight limitations. Two shaped charges were fabricated for the March 1978 launches. With Wallops Flight Center assistance modification was made to our payload design to accommodate the charge and two payloads were built.

With a viable lightweight payload and optimized tapering cone shaped charge developed, the emphasis of the program turned to the scientific goals.

We proposed to fire two Nike-Tomahawks into bright, discrete auroras to further investigate the formation, spacial and temporal evolution of laminar V-shocks (Swift et al., 1976). Our previous barium plasma injection experiment in conjunction with observations from Skylab (Wescott et al., 1976b) had produced the first direct evidence of a U-shaped double-layer or laminar V-shock at an altitude of about 1 $R_E$ over a discrete aurora (Figure 1). There were large perpendicular electric fields above that altitude, and small fields below, resulting in a shearing off and rapid dispersion of the barium flux tubes above, eventually leaving only the sheared off stub below. In retrospect we now think that the Oosik experiment (Wescott et al., 1975a) also encountered such a potential distribution below 2000 km altitude, Figure 2.

S3-3 satellite observations have shown many auroral zone passes with spatially confined regions of extremely large electric fields whose structure suggests paired electrostatic shock (V-shocks) located at altitudes between 1000 km and 8000 km (Mozer et al., 1977).

The barium plasma injection experiments have the advantage of allowing observation of parallel and perpendicular electric fields for thousands of km along a field line at the same time. Also if a U-shaped potential structure or V-shock develops in the region of a barium flux tube, the effects can be observed for a relatively long time. This is a great advantage compared with measurements from a satellite which moves across the structure at about 8 km/sec.

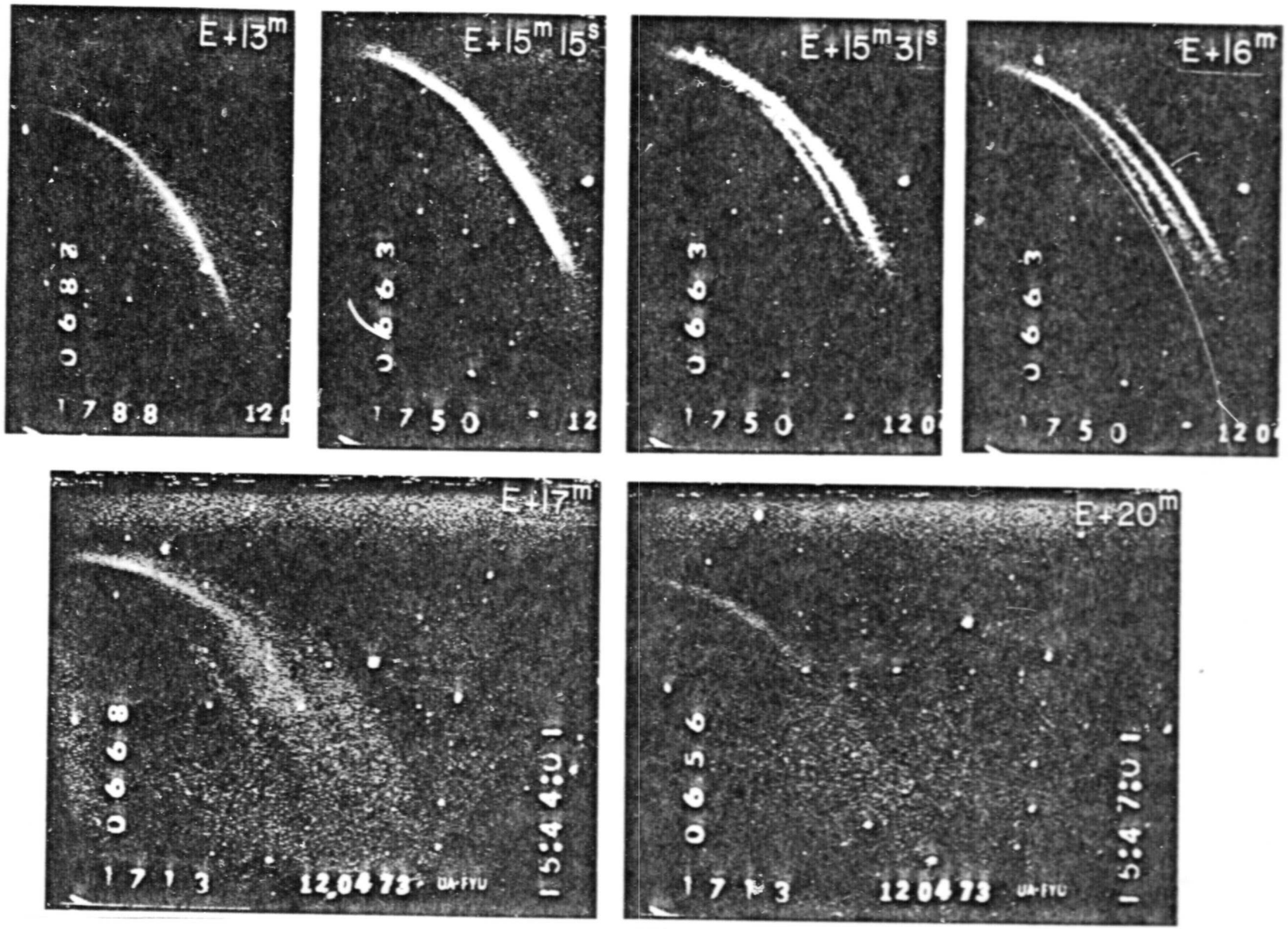


Figure 1. The encounter of the Skylab Beta barium flux tube with a laminar-V shock or U shaped double layer. In the upper left frame, at 13 minutes after injection, the streak is a single flux tube extending from 4500 km altitude at upper left to near 10,500 km altitude near center right. From E+15m 15s the streak brightened rapidly to 3X its original value (next frame). The third frame shows the evolution of the first of several seperate streaks which seperated at high velocity above 5700 km altitude. The E+16m frame shows the lack of low altitude continuation of the sheared off streaks. The bottom two full frames show the continued rapid diffusion of the upper barium streaks to undetectability at E+20m.

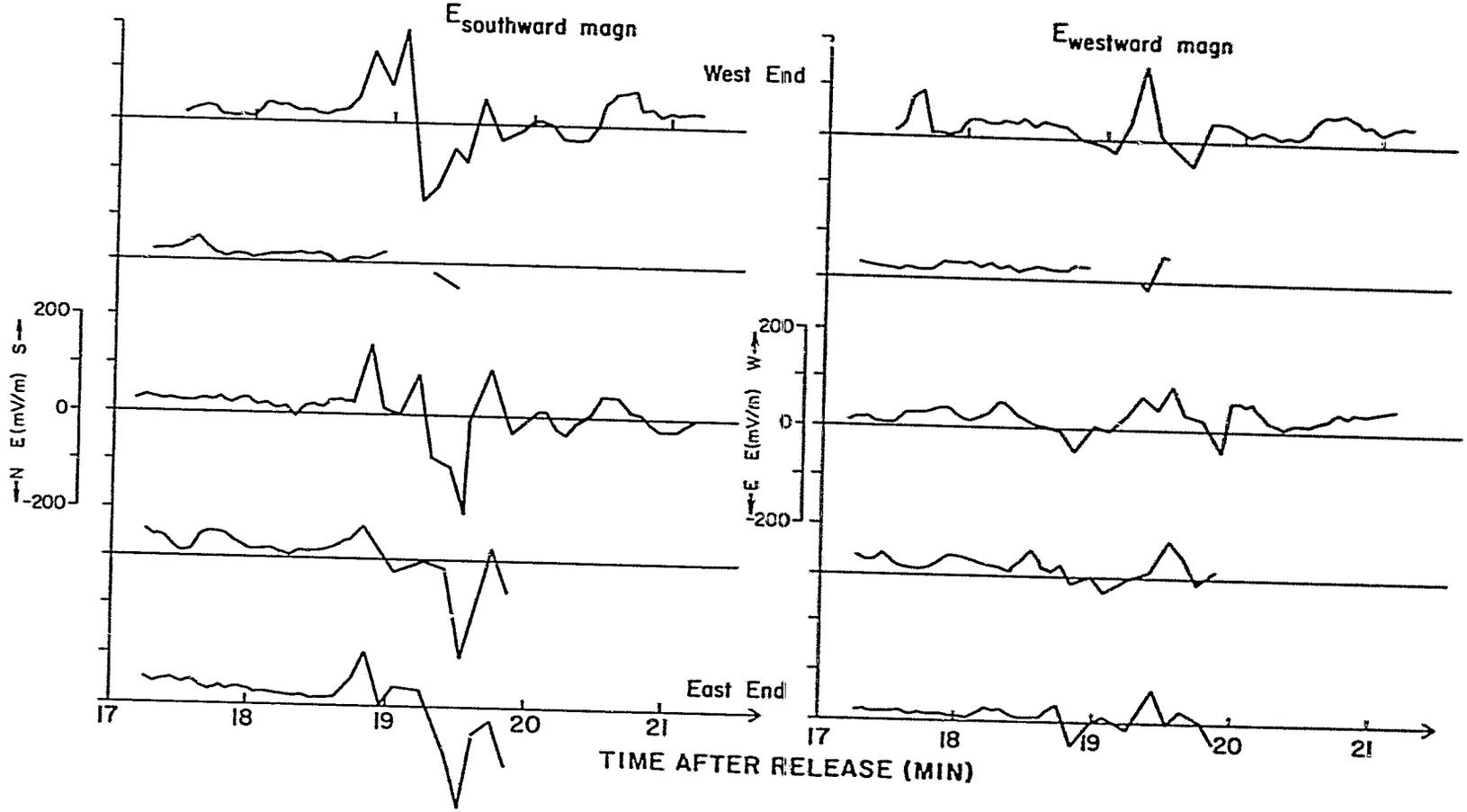


Figure 2. North-south and east-west electric field components referenced to 100 km altitude for the March 7, 1972 Oosik barium plasma injection experiment. Five separate principal plasma flux tubes are represented during the time a classic auroral spiral passed across the barium. The electric fields are characteristic of those found above a laminar V-shock associated with some auroras.

Nike-Tomahawk rocket 18.1018 UE was successfully launched from Poker Flat on February 27, 1978 into a promising auroral situtation. Detonation occurred near 450 km altitude, 100 seconds bright (> 100 kR in 5577 Å) auroral surge passed across the barium flux tube (Figure 3). We found no evidence of any large perpendicular or parallel electric fields associated with the discrete aurora below about 1700 km. Lack of rapid internal shear motions in the TV all-sky camera data suggest that no laminar V-shock existed above the aurora in this case.

Nine minutes later the upwards streaming plasma began to be decelerated, eventually stopping and falling back down the field lines. We have analyzed these exciting phenomena in a paper (Wescott et al., 1980), being submitted to JGR for publication and included as Appendix A to this report.

Nike-Tomahawk 18.1019 UE was successfully launched from Poker Flat on 10 March, 1978 into an active postbreakup auroral situation. Detonation occurred near 444 km altitude. The analysis of this flight is complete and a paper on the results is in preparation. The convection was typical of postbreakup auroral conditions with much larger electric fields evident than during 18.1018 UE.

Taurus Tomahawks 12.1003 UE and 12.1004 UE

The four previous Nike-Tomahawk flights conducted as part of the project were all successful, with apogees near 450 km. There were some difficulties in the wind-weighting due to lack of experience with such a lightweight payload. However, at 450 km altitude there are significant losses in a plasma injection due to collisions with the ambient atmosphere. The nominal minimum "no loss" altitude for detonation is considered to

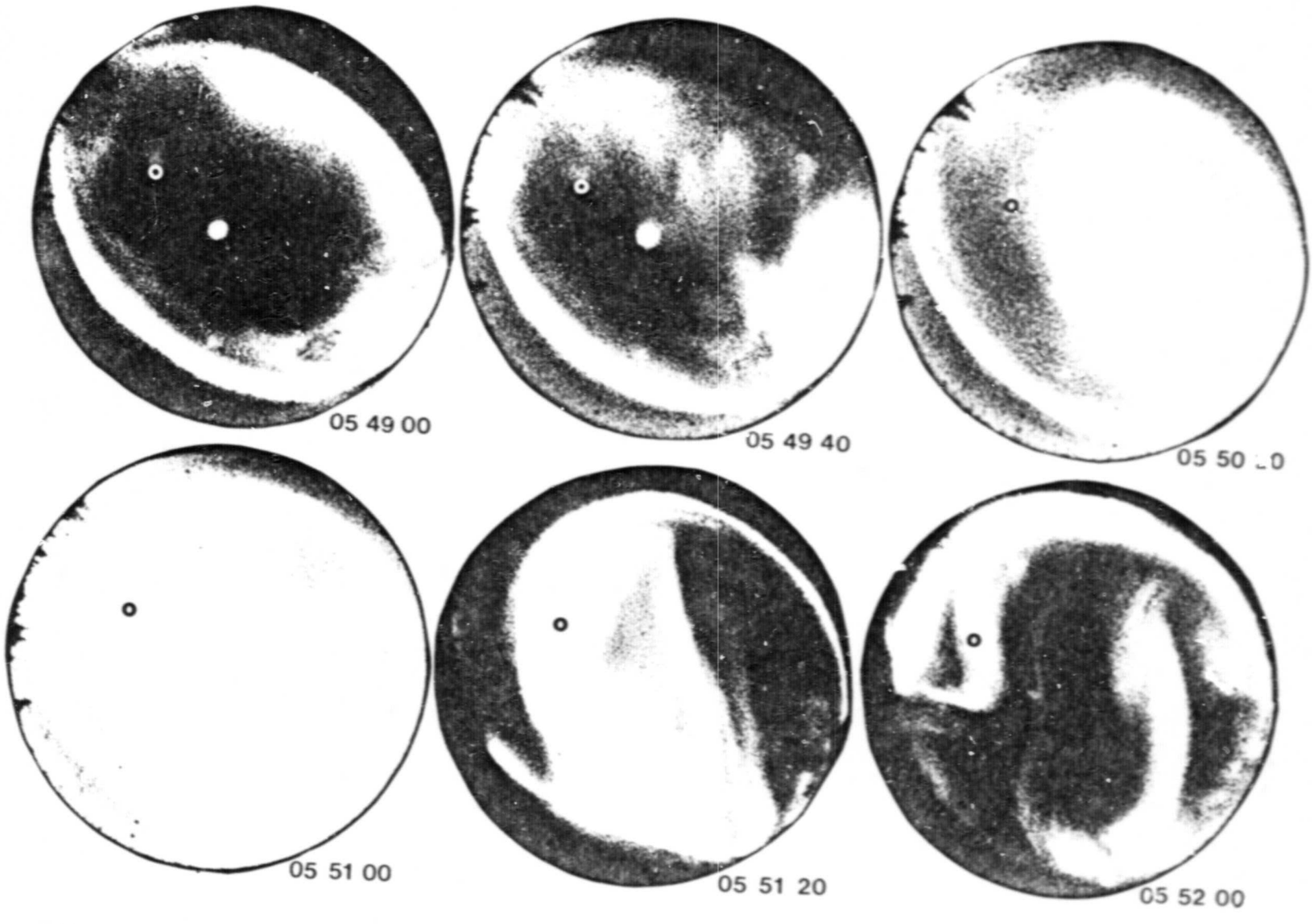


Figure 3. The Duchess barium plasma injection from Nike-Tomahawk 18.1018 UE. All-sky camera frames from Fort Yukon, Alaska, during the first three minutes are printed such that geographic north is up, east is to the right. The explosive debris and low-velocity barium ion cloud can be seen on several frames, and the field-line projection at 100 km altitude of the barium plasma flux tube is shown as an open circle.

be 500 km, so additional altitude performance was desired. The length of the launch window is also increased with additional altitude, allowing a better chance to launch into an auroral situation which promises substantial scientific results.

Therefore in 1978 James Gray of Wallops Flight Center suggested the use of an improved Honest-John rocket (called the Taurus) as the booster for the Tomahawk. Calculations showed that with our normal payload weight, an apogee altitude of 570 km could be achieved. This rocket combination was successfully test flown from Wallops Island with a payload similar to ours in weight and length.

We proposed to fly two Taurus-Tomahawk rockets with the proven payload in further experiments on the auroral acceleration process in discrete auroras. Because of the very great difficulties in shipping the high explosives and barium from Germany, we felt it was important to find a United States supplier for our shaped charges and cones. We negotiated with Thiokol Chemical Corporation to manufacture the shaped charges, and they located subcontractors to cast and machine the barium cones. We had four made for use in the program.

Taurus-Tomahawk rocket 12.1003 UE was successfully launched from Poker Flat on 27 March 1979. The detonation occurred at 1111:05 UT, at 65.86°N, 147.22°W, and 576.89 km altitude, polewards of a discrete arc. The aurora featured an upper height extent greater than those we have investigated in past years. There were long rays evident in the form. After initial rapid convection for several minutes, the auroral activity diminished, and we observed the barium streak and lower-end debris cloud for nearly two hours with very little motion, signifying near-zero

electric fields. We have completed sufficient analysis of this experiment to ascertain the electric fields and relationship to the aurora. There is no evidence of the barium and aurora coalescing on the same flux tube, and no evidence of unusual perpendicular or parallel electric fields characteristic of laminar V-shocks.

On 1 April 1979, Taurus-Tomahawk 12.1004 UE was successfully fired from Poker Flat. The plasma injection occurred at 1038:12 UT at 66.4529°N 146.2615°W, and 578.76 km altitude. There were multiple active arcs from north of Fort Yukon to south of the zenith at Poker Flat. The barium streak broke up into multiple striations in a few minutes. We were able to observe the ion debris cloud for over an hour, as the general convection was small. We have made preliminary analyses of the convection and auroral patterns but more detailed work is required. As far as we can tell, no laminar V-shocks were encountered.

We made observations of these two experiments from Poker Flat, Fort Yukon, Alaska, and from the NASA Learjet flying out of Ames Research Center. The TV from the Learjet observed 12.1004 UE for 18 minutes before the aircraft had to return to Ames. Figure 4 shows a photo mosaic of the plasma jet from the aircraft. In October of 1978 we also flew our TV system in the NASA Learjet in support of J. P. Heppner's satellite barium release program, CAMEO. Excellent data were obtained in a flight out of Fairbanks as shown in Figure 5.

Plasma Perturbation Experiments

We have conceived the idea of injecting barium plasma with azimuthal symmetry in a thin sheet perpendicular to the magnetic field. This would produce a significant perturbation to the magnetic field and to

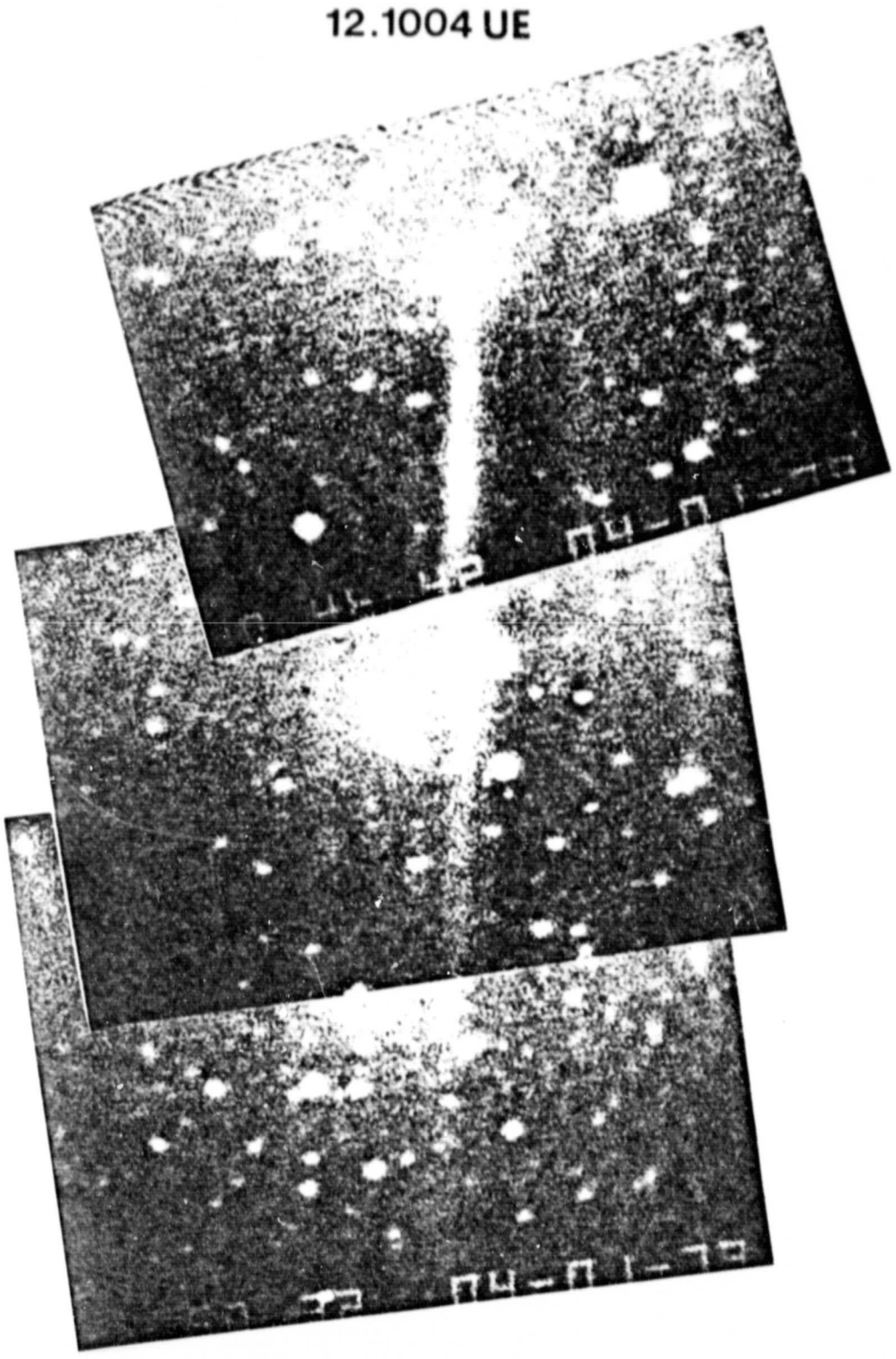




Figure 4. Photo mosaic of TV frames from the NASA Learjet flying near San Francisco, shows the barium jets produced over Poker Flat by rocket 12.1004 UE.

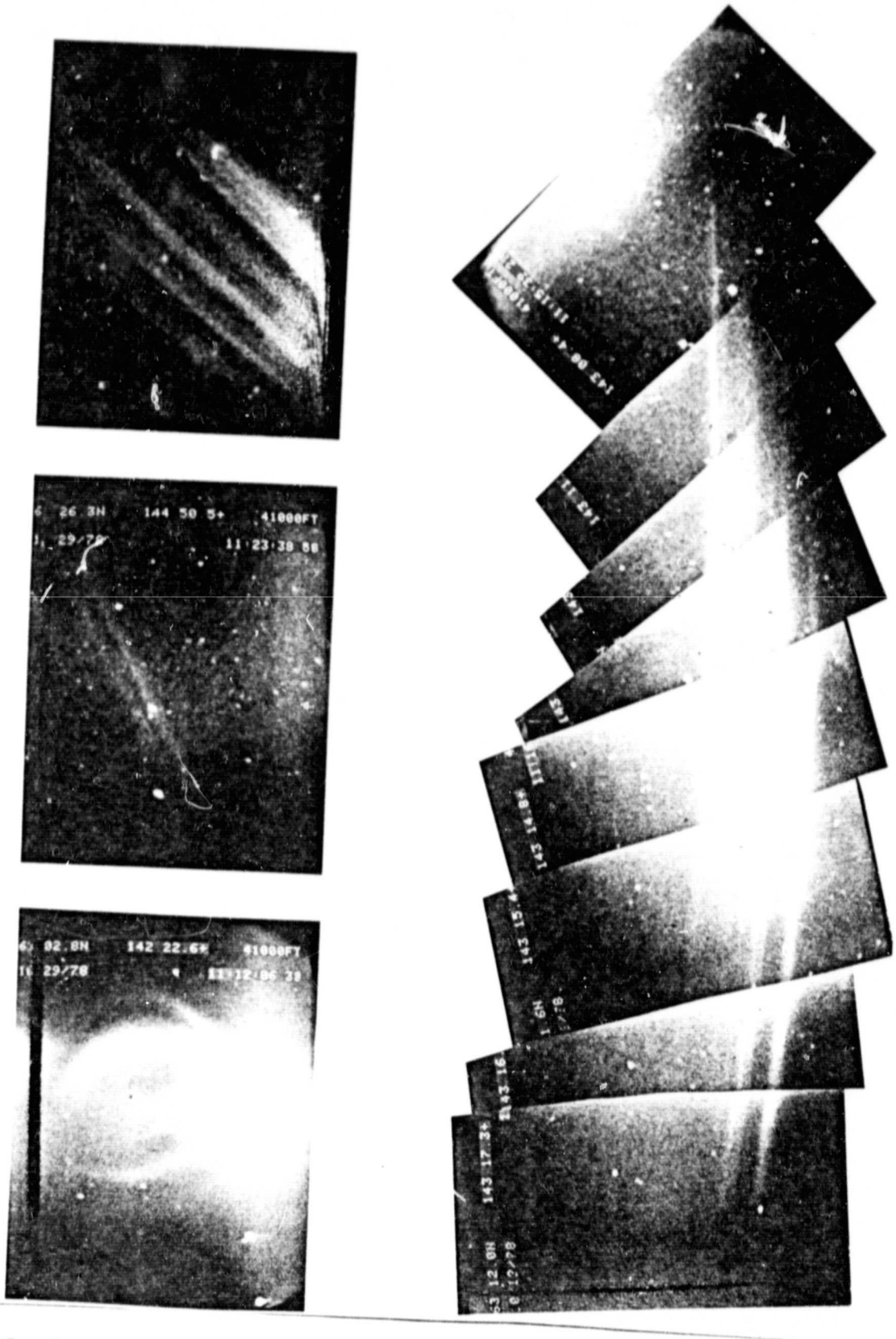

Figure 5. Photo mosaics of TV frames from the NASA Learjet flying over Alaska during Heppner's satellite barium release experiment, CAMEO.

the ambient waves and plasma. Our qualitative analysis of such an experiment suggests that a solenoidal electric field of near 500 mV/m would be produced in the first few tenths of a second by the transverse-streaming plasma. We predict that the propagation of this field to the ionosphere below, where conductivity becomes significant, would result in a solenoidal Pedersen current and a radial-inward Hall current. This suggests the possibility of energizing electrons to be precipitated into the ionosphere with observable optical and radio effects. We also predict the stimulation of pulsating aurora beneath the injection under the proper conditions as have been observed by Deehr and Romick (1977). VLF and ELF waves are also expected.

We designed a new type of radial shaped charge to carry out such an injection. Thiokol Chemical Corporation had made a policy decision not to continue this type of work, and no United States firm could be found who was willing to cast and machine the barium required. The previous shop where casting had taken place had been destroyed by fire during a procedure with lithium metal and was no longer in business. We developed our own facility for melting and casting barium metal slugs in an inert atmosphere and, after considerable effort and experimentation, learned how to make barium castings. However, we need to upgrade our capability to machine the barium into the required shapes. A radial shaped charge and barium liner are at this time nearly completed for a rocket experiment in March 1980. Los Alamos Scientific Laboratory kindly assisted in machining the barium slugs we made, and Falcon Research is fabricating the high-explosive shaped charges. We can expect Falcon Research to be a future source of the high-explosive shaped-charges, but machining of the barium slugs by Los Alamos Scientific Laboratories is in the

nature of a one-time favor for a scheduled March 1980 launch of the experiment. Future use of LASL for machine work is very uncertain.

We are well on shcedule for a March 1980 series of Taurus-Tomahawk launches from Poker Flat: two standard shaped-charge auroral laminar V-shock experiments and one radial shaped-charge perturbation experiment.

Papers presented at conferences

Davis, T. N., Optical observations of active experiments, presented at ARAKS Franco-Soviet Symposium, Toulouse, France, May 1976.

Davis, T. N., Optical observations of auroras and active experiments, AGU Chapman Conference at Yosemite, February 1976.

Haerendel, G., H. Föppl, E. Rieger, A. Valenzuela, H. C. Stenbaek-Nielsen, and E. M. Wescott, First observation of electrostatic acceleration of barium ions into the magnetosphere, Symposium on Active Experiments in Space Plasmas, Boulder, Colorado, June 3-5, 1976.

Haerendel, G., E. Rieger, A. Valenzuela, H. Föppl, and H. C. Stenbaek-Nielsen, First observation of electrostatic acceleration of barium ions into the magnetosphere, presented to ESO meeting, Schloss Elmau, Federal Republic of Germany, 1976.

Pongratz, M. B., W. B. Broste, and E. M. Wescott, Three-dimensional studies of magnetospheric cleft and polar cusp convection using shaped-charge barium injections, International Symposium on Solar-Terrestrial Physics, Boulder, Colorado, June 7-18, 1976.

Wescott, E. M., Review of barium shaped charge plasma injection experiments, Symposium on Active Experiments in Space Plasmas, Boulder, Colorado, June 3-5, 1976.

Wescott, E. M., T. Hallinan, and H. C. Stenbaek-Nielsen, Barium plasma injection experiments and laminar V-shocks above discrete auroras, Trans. Am. Geophys. Union, 60, 351, 1979.

Papers published or in press*

Davis, T. N., Chemical releases in the ionosphere, Reports on Progress in Physics, 42, 1565-1604, 1979.

Davis, T. N., W. N. Hess, M. C. Trichel, E. M. Wescott, T. J. Hallinan, H. C. Stenbaek-Nielsen, and E. M. Maier, Artificial aurora conjugate to a rocket-Borne electron accelerator, J. Geophys. Res., in press, 1980. (Attached as Appendix B)

Rieger, E., H. Föppl, G. Haerendel, A. Valenzuela, I. A. Zhulin, V. I. Gaidansky, V. S. Dokoulin, Yu. Ya. Ruzhin, and T. J. Hallinan, The barium ion jet experiment of Porcupine 2., Space Research, XIX, 367-371, 1979.

Swift, D. W., H. C. Stenbaek-Nielsen, and T. J. Hallinan, An equipotential model of auroral arcs, J. Geophys. Res., 81, 3931-3934, 1976.

Wescott, E. M., H. C. Stenbaek-Nielsen, T. N. Davis and H. M. Peek, The Skylab barium plasma injection experiments, Part I: Convection observations, J. Geophys. Res., 81, 4487-4494, 1976.

Wescott, E. M. H. C. Stenbaek-Nielsen, T. J. Hallinan, T. N. Davis, and H. M. Peek, The Skylab barium plasma injection experiments, Part II. Evidence for a double layer, J. Geophys. Res., 81, 4495-4502, 1976.

Wescott, E. M., H. C. Stenbaek-Nielsen, T. N. Davis, R. A. Jeffries, and W. H. Roach, The TORDO I polar cusp barium plasma injection experiment, J. Geophys. Res., 83, 1565-1575, 1978.

Winningham, J. D., D. S. Evans, E. W. Hones, Jr., R. A. Jeffries, W. H. Roach, T. W. Speiser, and H. C. Stenbaek-Nielsen, Rocket-borne particle measurements of the dayside cleft plasma: The TORDO experiments, J. Geophys. Res., 82, 1876-1888, 1977.

*Papers supported in whole or part by Grant NSG-6014, or publication costs paid for by NSG-6014 based on work performed under the previous rocket grant.

Papers being submitted for publication (See Appendix A)

Wescott, E. M., H. C. Stenbaek-Nielsen, T. J. Hallinan, and B. Häusler, Electric fields above a westward-travelling auroral surge and postsurge deceleration of barium plasma, for submission to J. Geophys. Res., 1980.

Papers in preparation

Murcray, W. B., T. N. Davis, H. C. Stenbaek-Nielsen, and E. M. Wescott, High-explosive detonations in the upper ionosphere. This paper is essentially completed, but submission is delayed pending receipt of original negatives from Los Alamos Scientific Laboratory for preparation of illustration.

Wescott, E. M., J. D. Stolarik, J. P. Heppner, G. J. Romick, D. D. Wallis, T. J. Hallinan, and H. C. Stenbaek-Nielsen. This paper is delayed because of a theoretical dispute between the co-authors on the existence of large inward directive electric fields at ionospheric heights. We may submit the observational results as a joint paper, followed by differing theoretical interpretations.

Wescott, E. M., Development of striations in barium plasma clouds, a counter example to the theory. Work on this paper is progressing nicely, and we expect to submit it for publication in the near future.

Wescott, E. M., H. C. Stenbaek-Nielsen, and T. J. Hallinan, Postbreakup auroral electric fields from a barium plasma experiment. Work on this paper is progressing also and we expect to submit it for publication in the near future.

## REFERENCES


Deehr, C., and G. Romick, Pulsating aurora induced by upper atmospheric barium releases, Nature, 267, 135, 1977.

Eichelburger, R. J., and E. M. Pugh, Experimental verification of the theory of jet formation by charges with lined conical cavities, J. Appl. Phys., 23(5), 1952.

Eichelburger, R. J., Re-examination of the nonsteady theory of jet formation by lined cavity-charges, J. Appl. Phys., 26(4), 398, 1955.

Jeffries, R. A., W. H. Roach, E. W. Hones, Jr., E. M. Wescott, H. C. Stenbaek-Nielsen, T. N. Davis, and J. D. Winningham, Two barium plasma injections into the northern magnetospheric cleft, Geophys. Res. Letter, 2, 285-288, 1975.

Mozer, F. A., C. W. Carlson, M. K. Hudson, R. B. Torbert, B. Parady, J. Yatteau, and M. C. Kelley, Observations of paired electrostatic shocks in the polar magnetosphere, Phys. Rev. Lett., 38, 292, 1977.

Rieger, E., H. Föppl, G. Haerendel, A. Valenzuela, I. A. Zhulin, V. I. Gaidansky, V. S. Dokaukin, Yu. Ya. Ruzhin, and T. J. Hallinan, The barium ion jet experiment of Porcupine 2., Space Research, XIX, 367-371, 1979.

Swift, D. W., H. C. Stenbaek-Nielsen, and T. J. Hallinan, An equipotential model of auroral arcs, J. Geophys. Res., 81, 3931-3934, 1976.

Wescott, E. M., H. M. Peek, H. C. Stenbaek-Nielsen, W. B. Murcray, R. T. Jensen, and T. N. Davis, Two successful geomagnetic field line tracing experiments, J. Geophys. Res., 77, 2982-2986, 1972.

Wescott, E. M., E. P. Rieger, H. C. Stenbaek-Nielsen, T. N. Davis, H. M. Peek, and P. J. Bottoms, L = 1.24 conjugate magnetic field line tracing experiment with barium shaped charges, J. Geophys. Res., 79, 159-168, 1974.

Wescott, E. M., H. C. Stenbaek-Nielsen, T. N. Davis, W. B. Murcray, H. M. Peek, and P. J. Bottoms, The L = 6.6 Oosik barium plasma injection experiment and magnetic storm of March 7, 1972, J. Geophys. Res., 80, 951-968, 1975.

Wescott, E. M. E. P. Rieger, H. C. Stenbaek-Nielsen, T. N. Davis, H. M. Peek, and P. J. Bottoms, The L = 6.7 quiet time barium shaped charge injection experiment "Chachalaca," J. Geophys. Res., 80, 2738-2745, 1975.

Wescott, E. M., H. C. Stenbaek-Nielsen, T. N. Davis, and H. M. Peek, The Skylab barium plasma injection experiments, Part I: Convection observations, J. Geophys. Res., 81, 4487-4494, 1976.

Wescott, E. M., H. C. Stenbaek-Nielsen, The Skylab barium plasma injection experiments, Part II: Evidence for a double layer, J. Geophys. Res., 81, 4495-4502, 1976.

Wescott, E. M., H. C. Stenbaek-Nielsen, T. N. Davis, R. A. Jeffries, and W. H. Roach, The TORDO I polar cusp barium plasma injection experiment, J. Geophys. Res., 83, 1565-1575, 1978.

Wescott, E. M., H. C. Stenbaek-Nielsen, T. J. Hallinan, and B. Häusler, Electric fields above a westward-travelling surge and postsurge deceleration of barium plasma, submitted to J. Geophys. Res., 1980.

Winningham, J. D., D. S. Evans, E. W. Hones, Jr., R. A. Jeffries, W. H. Roach, T. W. Speiser, and H. C. Stenbaek-Nielsen, Rocket-borne particle measurements of the dayside cleft plasma: The TORDO experiments, J. Geophys. Res., 82, 1876-1888, 1977.

APPENDIX A

# Electric Fields above a Westward-Travelling Auroral Surge and Postsurge Deceleration of Barium Plasma

Eugene M. Wescott, Hans C. Stenbaek-Nielsen, and Thomas J. Hallinan

Geophysical Institute, Fairbanks, Alaska 99701

Bernd Häusler

Max-Planck-Institut für Physik und Astrophysik

Garching b. München, Federal Republic of Germany

## ABSTRACT

On February 27, 1978, a barium shaped-charge experiment named "The Duchess" was carried out from Poker Flat, Alaska. The purpose of the experiment was to investigate U-shaped potential or laminar V-shock structures associated with discrete auroras. Injection occurred $1^m\ 40^s$ before a bright (> 100 kR in 5577 Å), westward-travelling auroral surge intersected the flux tube loaded with the barium plasma. The observed initial speed and direction of the neutral barium plasma with respect to the magnetic field and the field-aligned ion velocity are inconsistent with adiabatic motion. During the auroral encounter, the drift perpendicular to the magnetic field of the upwards-streaming plasma was slow, implying low $E_\perp$ and there was no detectable parallel field to an altitude of about 1700 km. All-sky TV pictures do not show any of the shear motions in the aurora indicative of the presence of a laminar V-shock; thus, in general, the evidence leads us to believe that the aurora did not have such a potential structure associated with it.

Nine minutes after the passage of the surge, the field-aligned motion of the barium plasma began to decelerate from its initial velocity of 13 km/sec. Within a few minutes the plasma stopped its upwards motion and began to fall back down the magnetic field line. Down-field line directed electric fields of 98 μV/m for 1.6 minutes and then 5 μV/m for 10 minutes are suggested by the observations; however, a beam plasma interaction with the ambient plasma might be involved.

## Introduction

Fast barium plasma injected parallel to the magnetic field above the atmosphere and in sunlight serves as a fluorescent tracer of magnetic and electric fields. From ground or aircraft stations located in darkness the plasma can often be followed many thousands of kilometers out into the magnetosphere. A number of such experiments, conducted in the auroral zone, have revealed important facts concerning the perpendicular and parallel electric fields associated with auroras (Wescott et al., 1975, 1976; Haerendel et al., 1976).

As a continuation of our experiments in auroral acceleration mechanisms, we developed a lightweight payload (60 pounds) which could be lifted to 450 km on a Nike-Tomahawk rocket. Wallops Flight Center cooperated in the design and construction of the payload hardware, and the Max-Planck-Institut für extraterrische Physik cooperated in the design and construction of a barium shaped charge for the lightweight payload.

On February 27, 1978, a barium shaped-charge payload named "The Duchess" was launched on NASA Nike-Tomahawk rocket (18.1018 UE) from Poker Flat, Alaska, in active auroral conditions. The detonation occurred at 0549:00 UT (1830 magnetic local time) near 450 km. The primary goal of the experiment was to determine the temporal and spatial evolution of laminar V-shocks, or potential double layers over a discrete aurora (Swift et al., 1976).

For an optimum barium plasma experiment it is necessary to launch the rocket at least six minutes, and ideally about 20 minutes, before the aurora crosses into the L shell of the injection. In "The Duchess" experiment the auroral activation developed more rapidly than we expected after the launch, and a bright (> 100 kR in 5577 Å) westward-travelling auroral surge

passed through the barium before it was very far into the magnetosphere. There were three unusual effects seen during the observations: 1) From the observed injection angle and the up field-aligned motion, it appears that a non-adiabatic process was involved; 2) below about 1700 km altitude there was a complete lack of any electric field effect due to the auroral surge; 3) an unusual deceleration of the barium plasma parallel to the magnetic field occurred in the post-breakup aurora.

The geophysical environment of the experiment

Some Planetary magnetic indices are given in Table 1 below. There was moderate magnetic activity before and during the experiment.

TABLE 1

Planetary Indices, February 27, 1978

| Time UT | 04 | 05 | 06 |
|---|---|---|---|
| Dst(nT) | -45 | -48 | -52 |
| Kp | | 4+ | |
| SOLAR FLUX 2300 MHz (Sa) | | 137.5 | |
| IMF | | AWAY | |

Figure 1 shows some selected H component magnetograms for February 27, 1978. The plasma injection occurred at 0549:00 UT during a positive H excursion at College which reached a maximum of about 200 nT two minutes after injection, followed within 10 minutes by a 100 nT negative bay in H.

Figure 2 shows all-sky camera frames from Fort Yukon, Alaska (66°33.6'N, 145°13'W) which is located nearly beneath the barium release. The release occurred at 0549:00 UT between two discrete arcs. At the time of the release there were three arc systems over central Alaska, the brightest of which, in the south, was 32 kR in 5577 Å as seen from Poker Flat. A westward-travelling surge with a brightness of about 135 kR in 5577 Å in the most poleward arc moved across the barium flux tube about 1 minute 40 seconds after the injection. Figure 3 shows the mapped auroral positions and the 100 km intercept of the brightest barium flux tube for the first three minutes after the injection.

Observational technique and data analysis

Sensitive image orthicon TV cameras operated at several Alaskan sites provided the primary data base for determining the position in space of the fluorescent barium ions. Cameras were located at the Geophysical Institute building in Fairbanks (64.886°N, 147.847°W), the Ester Dome Observatory (64.880°N, 148.053°W), and Kotzebue (66.883°N, 162.633°W). The cameras were fitted with f/0.75, Olde Delfte lenses and after one minute were operated with a 25 Å wide interference filter centered on the 4554 Å line of ionized barium. For late-time sensitivity they could be used in an integration mode for exposures of up to eight seconds.

Additionally, an all-sky SIT Videcon TV was operated at the Poker Flat Research Range (65.1168°N, 147.464°W). The auroral morphology was determined from 35 mm film all-sky cameras operated at Poker Flat, Ft. Yukon (66.56°N, 145.217°W), and Tok (63.33°N, 142.98°W).

The position of the detonation was obtained by triangulation between TV images against the star background from all the sites. The Ester Dome-Institute base line is 10.0 km, which is too short for triangulation beyond a few minutes of time. Due to sudden deterioration of the weather at Kotzebue only a few minutes of usable data were obtained from there. Thus we were forced to use a data reduction method that consisted of computing model field lines in astronomical coordinates for iterative comparison with the barium streaks observed from Ester Dome and the Geophysical Institute building against the star background. Additional information was obtained from the all-sky TV and camera observations of the low-altitude barium debris cloud. In order to be considered as an acceptable fit to the data, a theoretical field line had to thread through the lower-end debris cloud as well as the portion of the streak far out along the field line.

The magnetic field model used was POGO 10/68 (Cain and Cain, 1971) and the Mead-Fairfield external coefficient field (Mead and Fairfield, 1973). In the auroral conditions of this experiment it was also necessary to allow for the effects of parallel current sheets which produce a skewing effect on the magnetic field. The model incorporated an infinite current sheet aligned at any selected angle with respect to L, with current upwards either polewards or equatorwards of the barium, and with current density dependent upon distance along the field line to take the divergence of the field into account.

In general, triangulations or field-line determinations were made at one-minute intervals except where closer time resolution was needed. At late times the barium streaks became too diffuse for good position

determinations probably due to motion during the integration. There were, however, several late-time intervals when the barium suddenly became sharply defined. The last sharp barium streak which could be accurately located was at 0622, or 33 minutes after the injection.

All positional data are given on a 100-km datum map surface for direct comparison with auroral features. This was accomplished by field line tracing downwards along the model field lines to 100 km altitude.

Observations of the convection electric fields in an auroral surge

Figure 3 shows the mapped positions of the auroral lower borders and the brightest barium streak for the first three minutes of the experiment. Figure 2 shows the all-sky camera frames from Ft. Yukon (essentially under the barium) for the same period of time. At the burst time the barium was between discrete arcs (0549:00 UT). In 40 seconds a brightening of the aurora, which could be seen off to the east, became an evident westward-travelling surge in the form of a large backwards S. The bright edge of the surge passed across the barium flux tube circa 1 minute 40 seconds after release (0550:40) UT.

The up-field initial velocity of the tip of the barium jet was measured during the first 90 seconds as 13.0 km/second. This value is high considering the injection angle, observed neutral velocity, and the effects of the magnetic mirror force as discussed later. Using this initial velocity, and integrating the equation of motion along the field line to account for deceleration due to gravity, puts the tip of the plasma at $1^m\ 40^s$ at 1674 km altitude. Plasma with lower field-aligned velocities was of course distributed between the tip and the burst point.

Eager eyes watched the TV monitors in real time and extensively reviewed the tapes later. The unanimous conclusion was that nothing happened when the bright surge crossed through the barium-laden field line. The average horizontal drift rate in the first $1^m\ 40^s$ was small, and it was still very small as the aurora crossed the field line. During the next five minutes the sky was filled with moving forms, but there was no discernible effect on the barium due to the presence of the auroral forms.

Figure 4 shows the 100 km projected track of the barium during the period of the observations. Figure 5 is a plot of the calculated total perpendicular electric field as determined from the barium velocity and also as determined from ion drift velocities determined from the Chatanika Radar (M. McCready and J. Kelley, private communication).

In some other instances of barium-aurora encounters, it has been possible to calculate the parallel current sheet in the aurora from the change in flux tube orientation before and after the encounter. At this early time in our experiment the length of flux tube which could be observed was short, which severely limited the amplitude of a current sheet crossing which could be detected; we estimate that the limit was 0.5 A/m.

Nearly eight minutes after the injection (0557:00 UT) a classic spiral auroral form passed near the barium as shown in Figures 6 and 7. We also examined the TV fields before and after this time carefully, but could not detect any change in the orientation of the barium flux tube.

We did find it necessary to use various parallel currents in order to match the barium streaks to the model when the aurora was present. Table 2 shows the 100 km amplitude of the model current sheet. In this experiment all sheet currents were oriented parallel to L, and all upwards currents were polewards of the barium. Equivalent downward current sheets would be equatorward of the barium. For the first 11 minutes of the experiment, the model current sheet required to fit the barium streak was large, about 0.4 A/m. As the auroral activity waned and the discrete forms retreated polewards, the current diminished to zero as shown in Table 2.

TABLE 2

| Time UT | Time After Burst (min) | Current Density A/m |
|---|---|---|
| 0553 | 4 | 0.40 |
| 0554 | 5 | 0.40 |
| 0556 | 7 | 0.40 |
| 0559 | 10 | 0.40 |
| 0600 | 11 | 0.30 |
| 0601 | 12 | 0.15 |
| 0603 | 14 | 0.10 |
| 0604 | 15 | 0.18 |
| 0605 | 16 | 0.05 |
| 0609 | 20 | 0.00 |
| 0615 | 26 | 0.00 |
| 0618 | 29 | 0.00 |
| 0622 | 33 | 0.00 |

Possible non-adiabatic processes in the injection

Differences between theoretical calculation of the upwards velocity parallel to the field vs time and observation of the neutral barium jet speed and injection angle with respect to the magnetic field lead us to suggest that a non-adiabatic process may occur in the early-time interval of the injection. The payload did not have an attitude control system, so that the angle of injection with respect to the ambient magnetic field direction depends upon the launch azimuth and elevation angles, the attitude of the rocket when it leaves the atmosphere, and the coning angle. As viewed from our TV station at Kotzebue, Alaska (66°53'N, 162°38'W) for the first 10 seconds, the neutral jet could be observed to be directed an apparent 22.5° above (or to the north of) the magnetic field direction. This is a minimum value, but probably close to the actual deviation since observations at two other stations, Geophysical Institute and Ester Dome, Alaska, (nearly in the plane of the magnetic field) did not distinguish any injection angle within a margin of about 5°. The apparent neutral velocity was 11.9 km/sec. The actual neutral velocity cannot be calculated because it depends critically on the angle in space and the viewing angle. However, the theoretical design parameters for the shaped charge predicted a peak velocity of 12.6 km/sec, and experience with other shaped-charge injections suggests that 13.0 km/sec is a reasonable value for the neutral velocity.

We have made calculations of the adiabatic motion (altitude and parallel velocity vs time) for a barium ion injected at the release point with various pitch angles and initial velocities. An injection of barium ions at the observed minimum angle of 22.5° with respect to the magnetic field, with an initial observed velocity parallel to

the field of 13.0 km/sec requires a minimum total initial velocity of 14.1 km/sec. This is unreasonably large. The ions behave non-adiabatically, i.e.: as if they are injected parallel to B even though the observations show the neutrals injected at a minimum angle of 22.5°. Therefore we suspect there was a non-adiabatic process to scatter ions towards smaller pitch angles, or to produce some acceleration parallel to the field. Similarly, for a large barium shaped charge experiment "Buaro" with injection perpendicular to the magnetic field, Pongratz and Jeffries (1976) reported that adiabatic ions could not travel up along B as fast as observed. They suggested that a wave plasma interaction occurred to stimulate pitch-angle diffusion into a direction parallel to B.

Deceleration of the barium plasma

When the tip of the barium streak can be located either by triangulation or by matching against a grid of model field lines, it is possible to calculate the adiabatic trajectory that an ion with initial velocity $v_o$ would take to reach the observed distance from the burst point in a given time. With an assumed $v_o$ and pitch angle, we calculated the instantaneous velocity vs time and altitude. Assuming no other influencing factors, such as parallel electric fields, $v_o$ should remain constant throughout the observations until very late times when we expect to observe the palpable tip retreat to lower altitudes due to the continued decrease in ion density and luminosity coupled with the threshold of detection of the TV systems. In Figure 8 we have plotted what the initial adiabatic velocity $v_o$ would have had to be in order to fit the observed tip of the plasma jet vs time. For 9 minutes $v_o$ is constant, near 13 km/sec, as expected. However, after 9 minutes there is a

significant decrease in $v_o$. This cannot be explained on the basis of the expected decrease in luminosity and TV sensitivity because: 1) the anomaly was observed early in the experiment; 2) the barium brightness was well above the threshold sensitivity of the TV, and the tip was relatively well defined, not diffuse. The deceleration can also be seen in a plot of altitude vs time as shown in Figure 9.

Parallel electric field calculation

Plasma experiments and theoretical work have shown instabilities and beam plasma interactions which might remove energy from a streaming plasma, slowing or stopping it. It may be that in the laboratory of space our observations are of such a nature. It is also possible that a parallel electric field, opposite to that which is thought to accelerate auroral electrons, is the cause of the barium deceleration. The barium is actually very sensitive to small parallel electric fields. The fast barium has an energy of about 100 eV/ion initially.

In 9 minutes the barium initially travelling at 13.0 km/sec was at an observed altitude of 6430 km, at which point it was travelling at the expected 10.7 km/sec due to gravitational slowdown. Ions with that velocity have an energy of 82 eV. After 9 minutes, it appears that the velocity of the ions (Figure 9) slowed down anomalously. In order to calculate the sort of parallel electric field required to duplicate the altitude vs time track (Figure 9), we calculated field-aligned ion motion applying various retarding electric fields. In Figure 9 we show the expected adiabatic trajectory with no parallel electric field and 13 km/sec initial velocity (dashed line). For instance, including a

small 7.5 μV/m constant field from time 0 (left side dotted curve, Figure 9) still does not make a good fit to the observed data (solid curves, Figure 9). We obtained a good fit with a -98 μV/m field applied for 1.6 minutes from 9 to 10.6 minutes after injection, then a -5 μV/m for the next 10 minutes (right side dotted curve, Figure 9). After that, the barium stops and falls back down the field line under gravity.

Such electric fields might be the result of a broad region of downward field-aligned current, or perhaps may represent large-scale turbulence equatorwards of the discrete aurora. Figure 6 illustrates the aurora as seen from Fort Yukon and the 100 km position of the barium flux tube. Figure 7 shows the mapped auroral positions. As the deceleration began, there were weakly scattered forms equatorwards of the bright discrete aurora. As the deceleration proceeded, the aurora faded further.

## Discussion

The fact that the observed initial parallel ion velocity cannot be reconciled adiabatically with the observed neutral velocity is suggestive of a pitch-angle scattering process or an early time acceleration. This has interesting connotations for perturbation experiments with plasma injected near perpendicular to the magnetic field.

On two previous occasions in barium plasma injection experiments, large electric fields characteristic of either a laminar V-shock or a potential double layer were seen when a discrete aurora passed through the barium flux tube. In the Oosik experiment (Wescott et al., 1975) as the polewards arm of a large spiral auroral form expanded and crossed

through a number of barium flux tubes distributed over several hundred kilometers along L, large (> 200 mV/km) electric fields which reversed direction were observed from 2000 km up to more than 10,000 km altitude. Though not recognized at the time, we now think this was an encounter with a laminar V-shock or potential double layer located below 2000 km altitude.

On the second experiment, Skylab Beta, (Wescott et al., 1976) again large perpendicular electric fields were seen as apparently a discrete auroral form crossed through the barium flux tube. On that occasion, however, the large fields were observed only above 5000 km with low fields below that. The result was a clear shearing effect near 5000 km, with eventual rapid dispersion of the barium ions above, leaving only the truncated barium streak below after the encounter. The authors concluded that this was clear evidence for a potential double layer or laminar V-shock near 5000 km altitude.

In the case of the present experiment we did not see any large electric field associated with the passage of the aurora. If a laminar V-shock or potential double layer existed on the auroral field lines, it was above 1700 km and did not affect the barium ions below. The aurora during this experiment was recorded with a television-type, all-sky camera and a review of the video tape shows that this aurora was totally devoid of the high-speed shear motions previously associated with laminar V-shocks. It is interesting to note that high values of $E_{\perp}$ (Hallinan and Davis, 1970) and U-shaped equipotential contours (Carlqvist and Boström, 1970) were both postulated initially on the basis of the observed high-speed internal ray motions in the aurora.

The third unusual observation during this experiment is the deceleration of the barium beginning 9 minutes after the injection. A possible mechanism could be that the free energy in the streaming plasma (of order 100 eV per ion) might be expended in a plasma instability. The fact that the last three points in Figure 9 fit a free-fall trajectory suggests that the barium plasma may have dissipated its kinetic energy through internal plasma instabilities. However, we have no other evidence that this happened, and in addition we have had many barium shaped charge experiments which did not indicate anything but gravitational deceleration. Further, there was nothing unusual in the auroral conditions at the time of the deceleration. Therefore, though we think that a plasma instability of some sort might decelerate barium ions, we cannot speculate on a specific instability.

The simpler explanation is that small parallel electric fields, as we have calculated, appeared and slowed the barium ions, eventually stopping their motion. The parallel field would have to be distributed along the length of the observed field line rather than concentrated at one altitude, such as in the case of a double layer, where pronounced change in the luminosity distribution would be observed.

Recently many satellite observations of electric fields, particles, and waves have been discussed in terms of electrostatic turbulence (Gurnett and Frank, 1977; Swift, 1977; Hudson et al., 1978; and Temerin, 1978, among others).

In the rest frame of the ambient plasma, Temerin (1978) reported that waves of near zero frequency are found with appreciable amplitude. The electric field parallel to the magnetic field, which we have suggested

could explain the deceleration, lasted the order of minutes. From the all-sky camera frames in Figure 6, one would best describe the aurora as patchy, disorganized, or perhaps even turbulent post surge. We suggest this may be evidence of large-scale electrostatic turbulence in the wake of the westward-travelling surge. Turbulence theory (Swift, 1979) implies potential differences in the magnetosphere which will be both positive and negative with respect to the ionosphere. Thus one would reasonably expect regions of both upwards and downwards current.

ACKNOWLEDGMENT

We wish to thank G. Haerendel of the Max-Planck-Institute for Extraterrestrial Physics for his help in producing the new shaped charge for this experiment. We are grateful to all the personnel at Wallops Flight Center who made the payload and suffered in the cold, launching the rocket, and in particular to Mendel Silbert, the Wallops payload manager. Mr. Louis Baim was the payload engineer for the Geophysical Institute who worked on the payload design and got it all together.

We also thank the crew of Poker Flat Research Range for a successful launch, and in particular Neal Brown, supervisor, and Mrs. Randi Wagner, who spent days on the telephone coordinating the explosives shipment. We are grateful to Mr. Garry Meltvedt of the Geophysical Institute who, in very adverse weather conditions, set up and operated our TV system at Kotzebue, Alaska.

We are indebted to the Defense Nuclear Agency and the USAF Alaskan Air Command for arranging the airshipment of the explosive shaped charges and barium from Germany.

The Geophysical Institute was work sponsored by a grant from NASA, NSG-6014.

## REFERENCES


Cain, J. C. and S. J. Cain, Derivation of the international geomagnetic reference field, NASA Technical Note D-6237, Goddard Space Flight Center, Greenbelt, MD, 1971.

Carlqvist, P. and R. Boström, Space-charge regions above the aurora, J. Geophys. Res. 75(34), 7140, 1970.

Gurnett, D. A., L. A. Frank, A region of intense plasma wave turbulence on auroral field lines J. Geophys. Res. 82, 1031, 1977.

Haerendel, G., H. Föpple, E. Rieger, A. Valenzuela, H. C. Stenbaek-Nielsen, and E. M. Wescott, First observations of electrostatic acceleration of barium ions into the magnetosphere, in European Programs on Sounding-Rocket and Balloon Research in the Auroral Zone, Rep. ESA-SP115, European Space Agency, Newilly, France, August 1976.

Hallinan, T. and T. N. Davis, Small scale auroral arc distortions, Planet. Space Sci., 18, 1735, 1970.

Hudson, M. K., R. L. Lysak, and F. S. Mozer, Magnetic field-aligned potential drops due to electrostatic ion cyclotron turbulence, Geophys. Res. Letters 5(2), 143, 1978.

Mead, D. M. and D. H. Fairfield, Quantitative magnetospheric models derived from spacecraft magnetometer data, Rep. X-641-73-363, Goddard Space Flight Center, Greenbelt, MD, 1973.

Pongratz, M. B. and R. A. Jeffries, A Buaro quick-look report, Los Alamos Scientific Laboratory, J-10-4227, 1976.

Swift, D. W., H. C. Stenbaek-Nielsen, and T. J. Hallinan, An equipotential model for auroral arcs, J. Geophys. Res., 81, 3931, 1976.

Swift, D. W., Turbulent generation of electrostatic fields in the magnetosphere, J. Geophys. Res. 82, 5143, 1977.

Swift, D. W., On the structure of auroral arcs: The results of numerical simulations, J. Geophys. Res., 84, 469-479, 1979.

Temerin, M., The polarization, frequency, and wavelengths of high-latitude turbulence, J. Geophys. Res. 83 (A6), 2609, 1978.

Wescott, E. M., H. C. Stenbaek-Nielsen, T. N. Davis, W. B. Murcray, H. M. Peek, and P. J. Bottoms, The L = 6.6 Cosik barium plasma injection experiment and magnetic storm of March 7, 1972, J. Geophys. Res., 80(7), 951, 1975.

Wescott, E. M., H. C. Stenbaek-Nielsen, T. J. Hallinan, T. N. Davis, and H. M. Peek, The Skylab barium plasma experiments, Part II. Evidence for a double layer, J. Geophys. Res. 81(25), 4495, 1976.

## FIGURE CAPTIONS

Figure 1. Selected H component magnetograms for February 27, 1978. "The Duchess" experiment began at 0549 UT.

Figure 2. All-sky camera frames from Ft. Yukon, Alaska, during the first three minutes of "The Duchess" experiment. The frames are printed such that geographic north is up, east is to the right, etc. The near zero velocity barium and explosive debris can be seen in several frames, and the projected position down the magnetic field line to 100 km is shown as an open circle.

Figure 3. Mapped auroral lower borders and the barium streak projected to 100 km for the interval corresponding to Figure 2. The arrow at the bottom indicates a drift velocity of 1 km/sec. All drifts during this interval were too small to show as a vector.

Figure 4. Track of the brightest barium streak projected down the magnetic field line to 100 km altitude.

Figure 5. Plot of the calculated total perpendicular electric field deduced from $\underline{E} = - \underline{v} \times \underline{B}$ of the brightest barium streak, referenced to 100 km altitude. The Chatanika radar electric field is shown as a broken line.

Figure 6. All-sky camera frames from Ft. Yukon, Alaska, during the interval when a deceleration of the barium took place.

Figure 7. Map projection to 100 km datum surface of auroral lower borders and the field line projected barium positions during the interval when the deceleration took place. The aurora was quite weak. The arrow at bottom indicates a drift velocity of 1 km/sec.

Figure 8. Calculated initial ballistic tip velocity, $v_o$, required for the barium to reach the observed altitude at the observed time. Under normal, zero parallel E field conditions, the plot of $v_o$ vs time would be a horizontal line (shown dashed) until late times. However, note the obvious deviation after 9 minutes as the apparent $v_o$ decreases.

Figure 9. Barium tip altitude vs time. The initial velocity was observed at 13.0 km/sec. To fit the deceleration curve, a parallel electric field of -98 μV/m is applied for 1.6 minutes, then a field of -5 μ/m for 10 minutes.

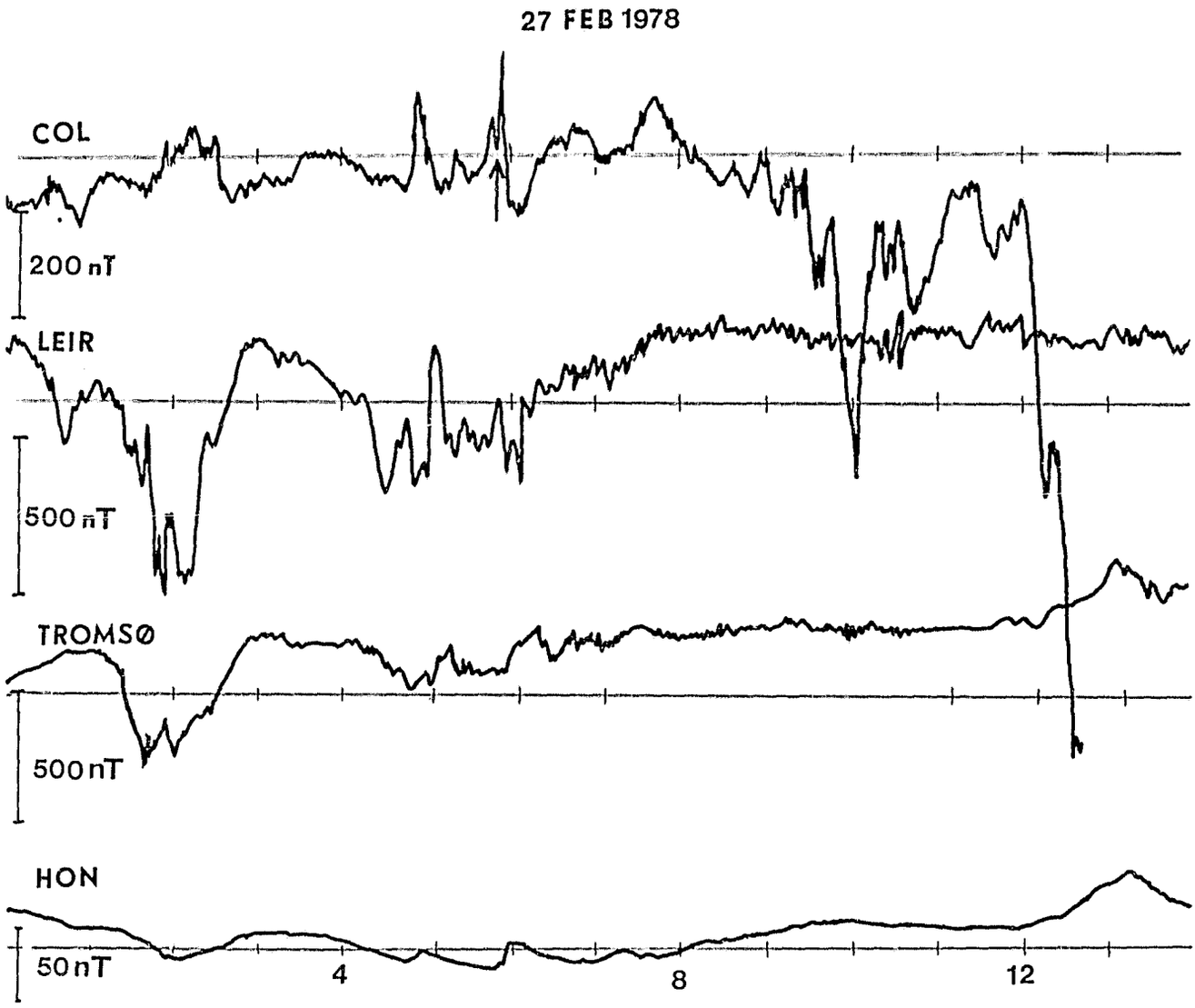


Figure 1. Selected H component magnetograms for February 27, 1978. "The Duchess" experiment began at 0549 UT.

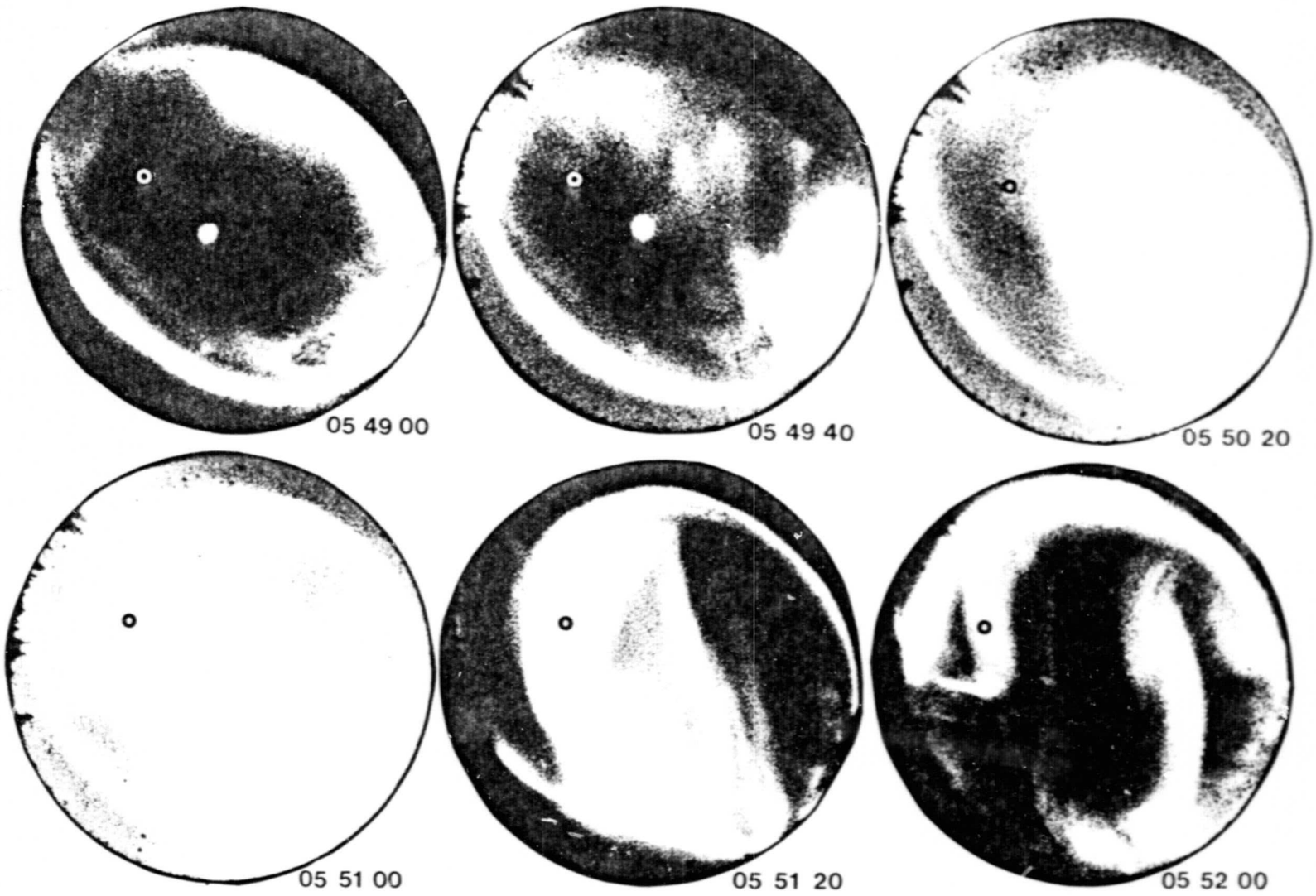


Figure 2. All-sky camera frames from Ft. Yukon, Alaska, during the first three minutes of "The Duchess" experiment. The frames are printed such that geographic north is up, east is to the right, etc. The near zero velocity barium and explosive debris can be seen in several frames, and the projected position down the magnetic field line to 100 km is shown as an open circle.

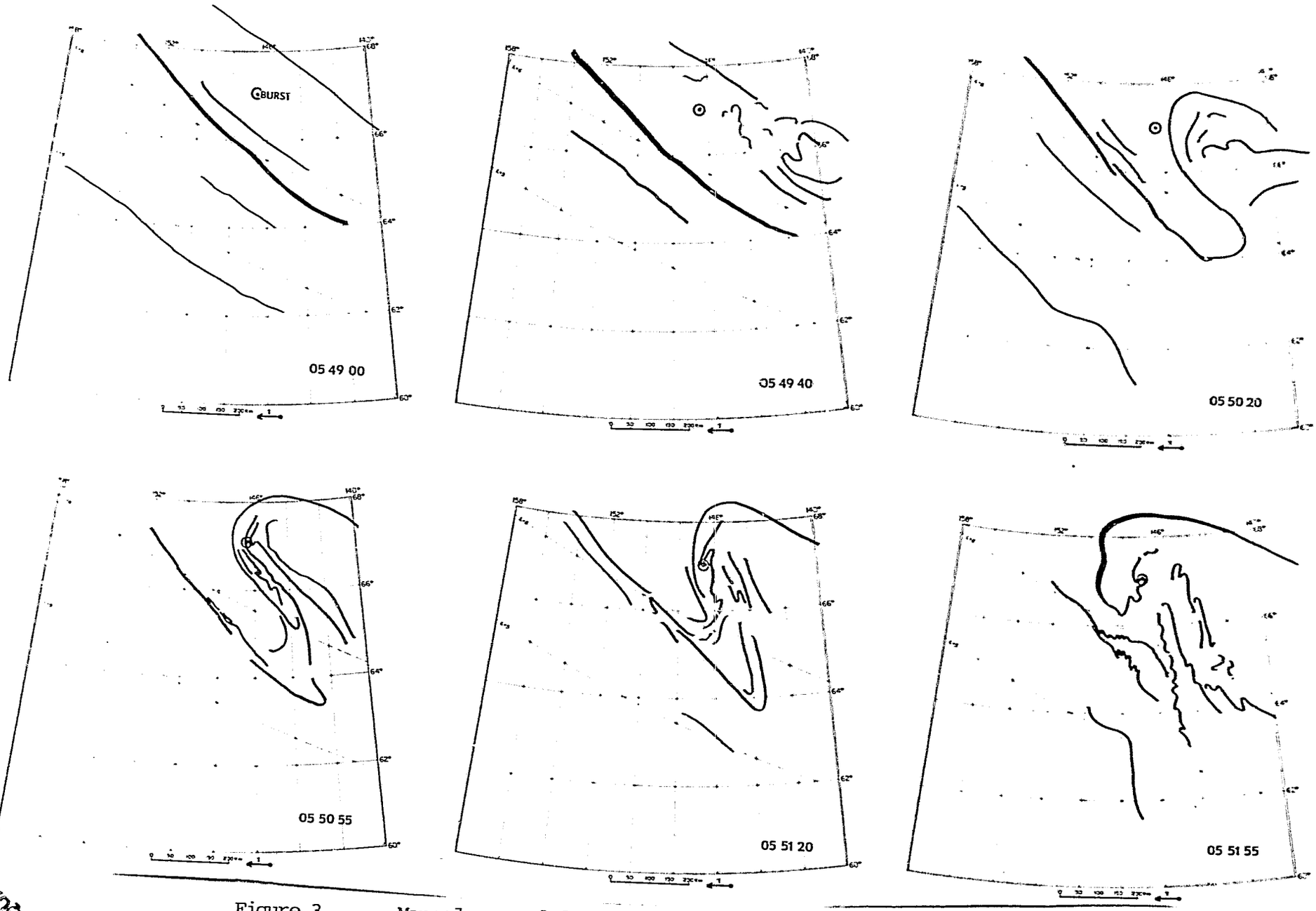


Figure 3. Mapped auroral lower borders and the barium streak projected to 100 km for the interval corresponding to Figure 2. The arrow at the bottom indicates a drift velocity of 1 km/sec. All drifts during this interval were too small to show as a vector.

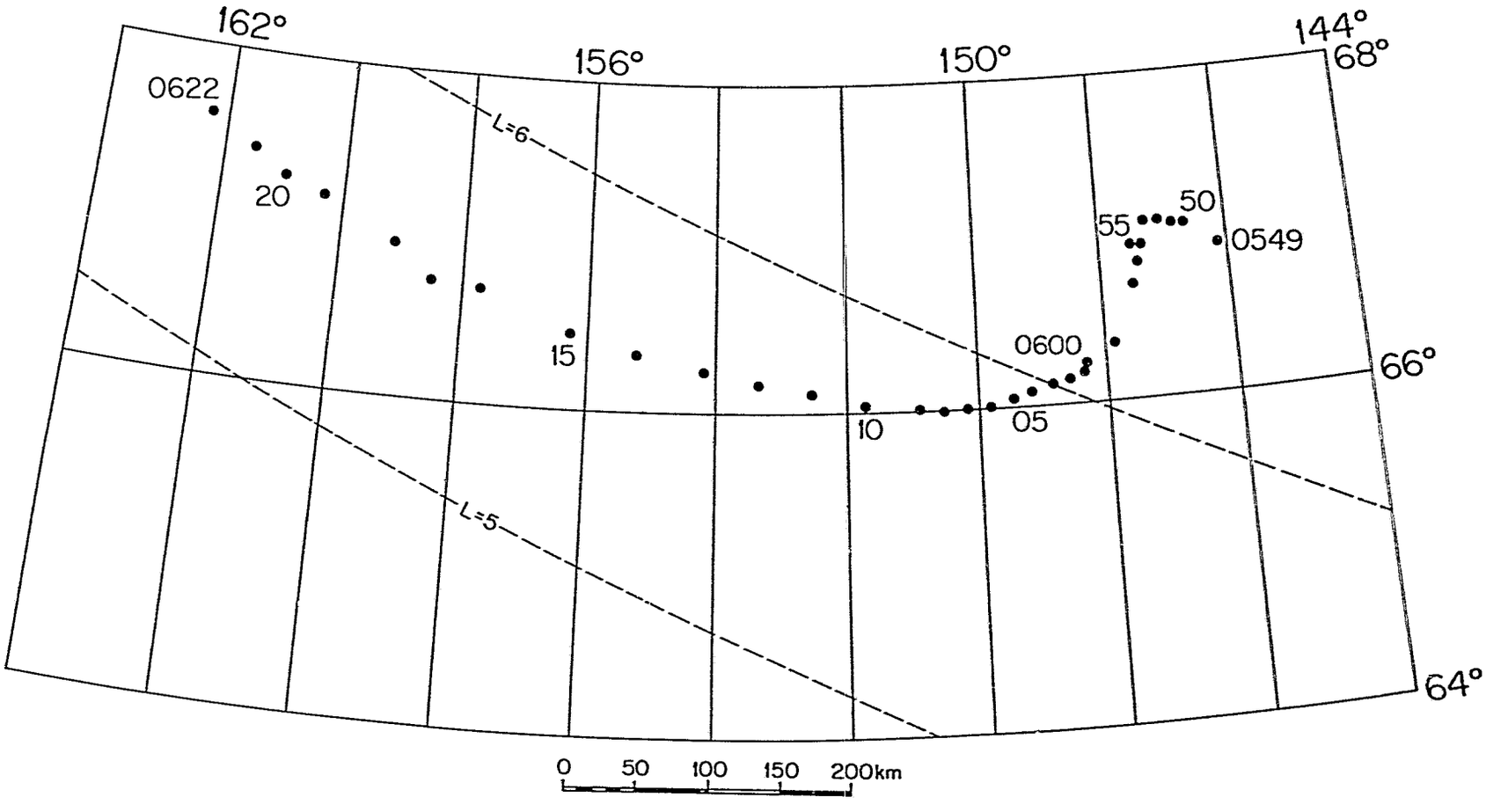


Figure 4. Track of the brightest barium streak projected down the magnetic field line to 100 km altitude.

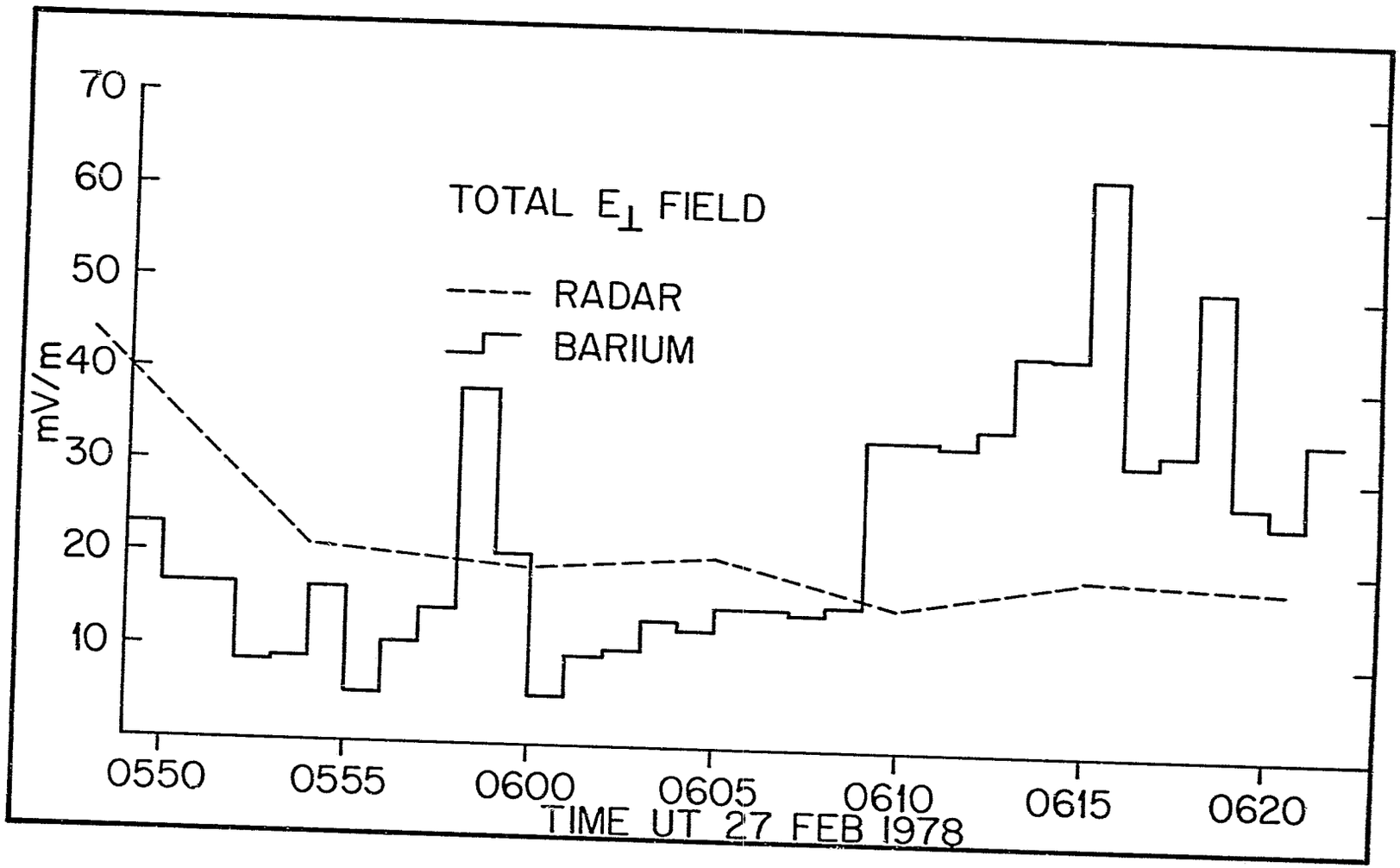


Figure 5. Plot of the calculated total perpendicular electric field deduced from $\underline{E} = - \underline{v} \times \underline{B}$ of the brightest barium streak, referenced to 100 km altitude. The Chatanika radar electric field is shown as a broken line.

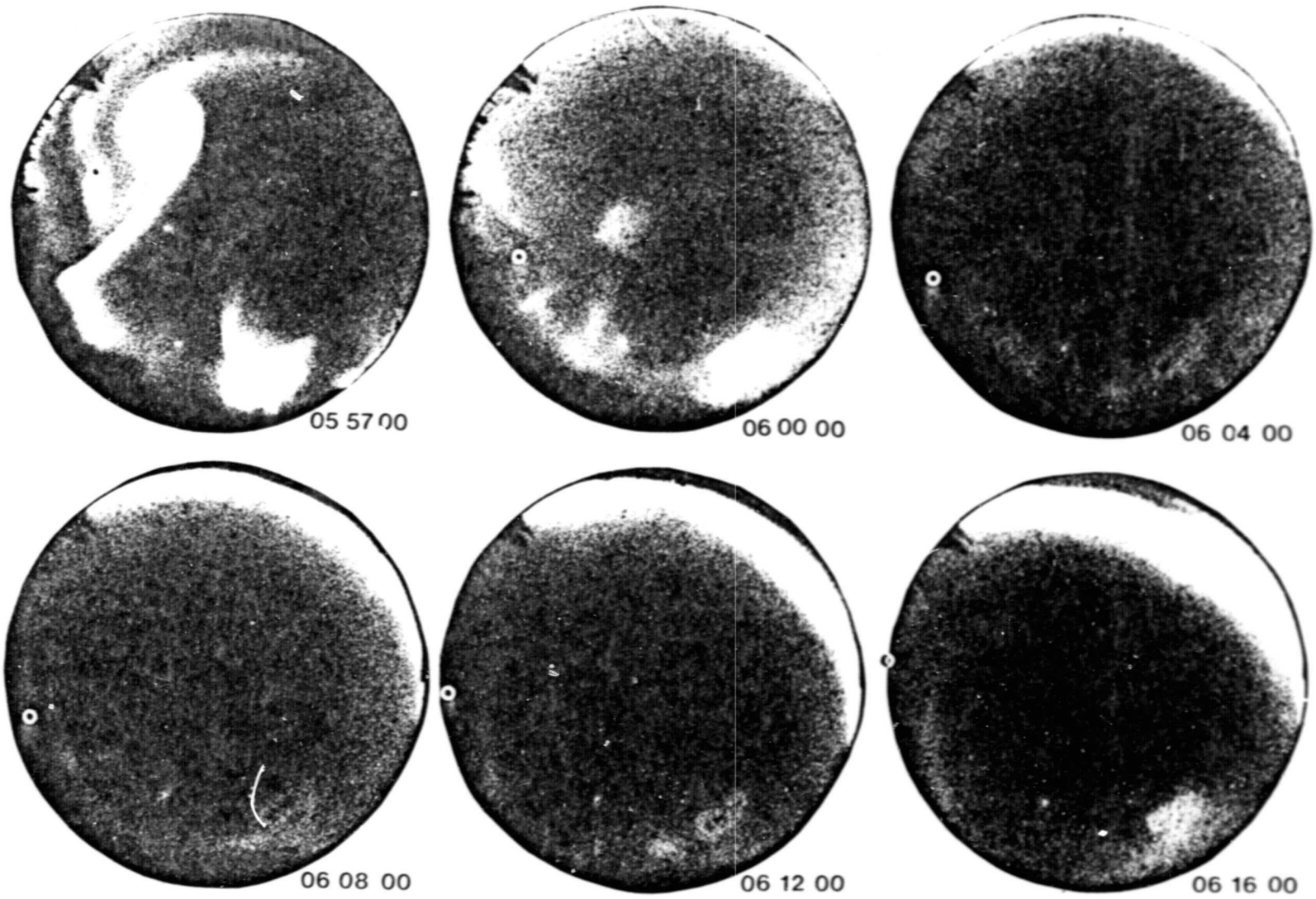


Figure 6. All-sky camera frames from Ft. Yukon, Alaska, during the interval when a deceleration of the barium took place.

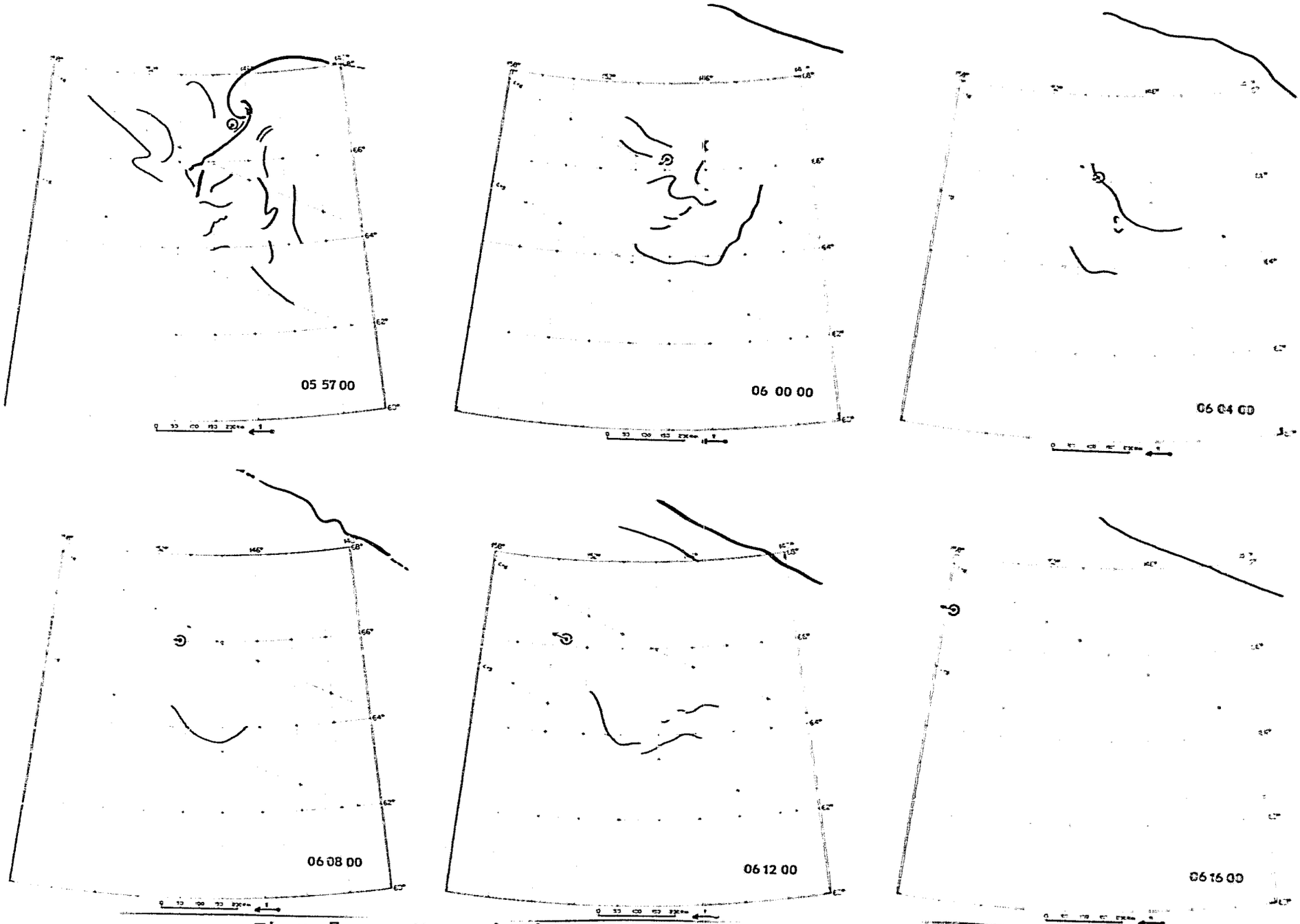


Figure 7. Map projection to 100 km datum surface of auroral lower borders and the field line projected barium positions during the interval when the deceleration took place. The aurora was quite weak. The arrow at bottom indicates a drift velocity of 1 km/sec.

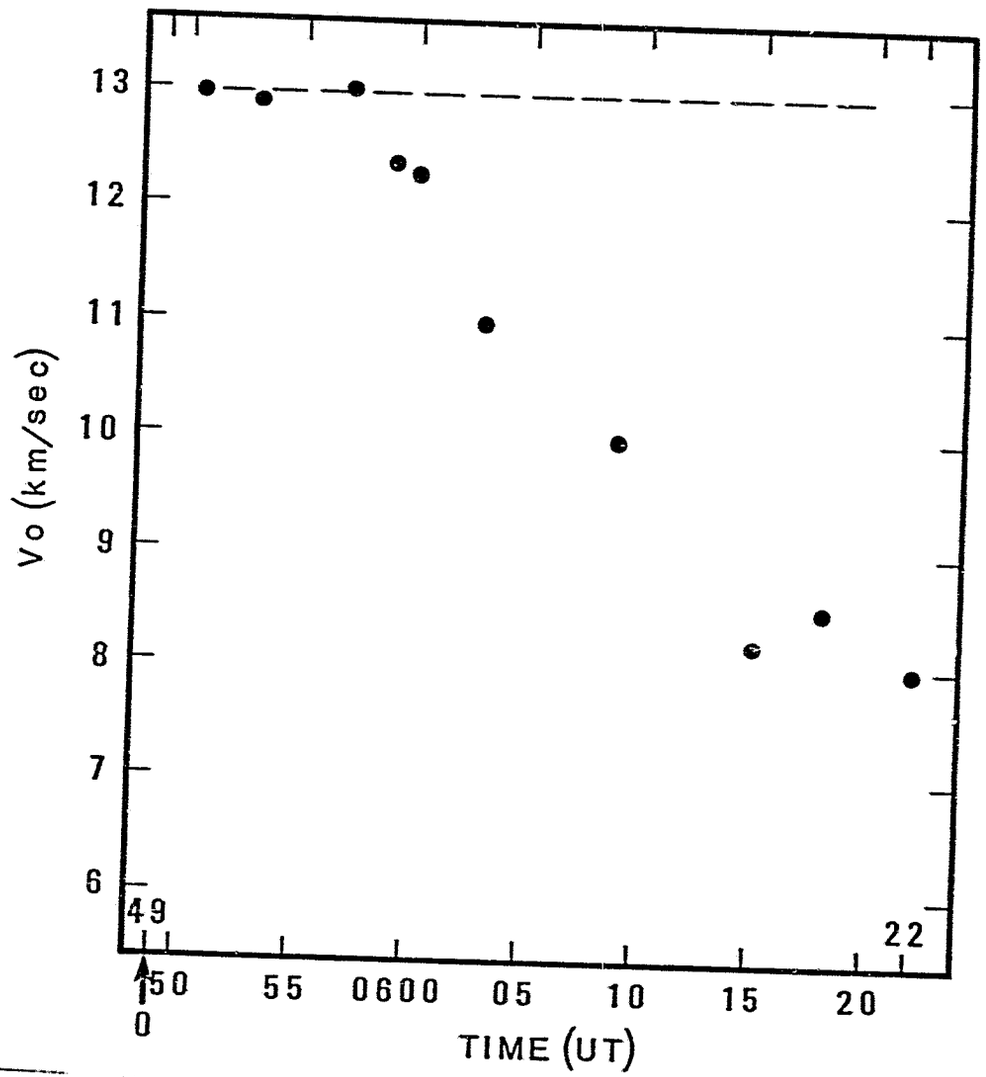


Figure 8. Calculated initial ballistic tip velocity, $v_o$, required for the barium to reach the observed altitude at the observed time. Under normal, zero parallel E field conditions, the plot of $v_o$ vs time would be a horizontal line (shown dashed) until late times. However, note the obvious deviation after 9 minutes as the apparent $v_o$ decreases.

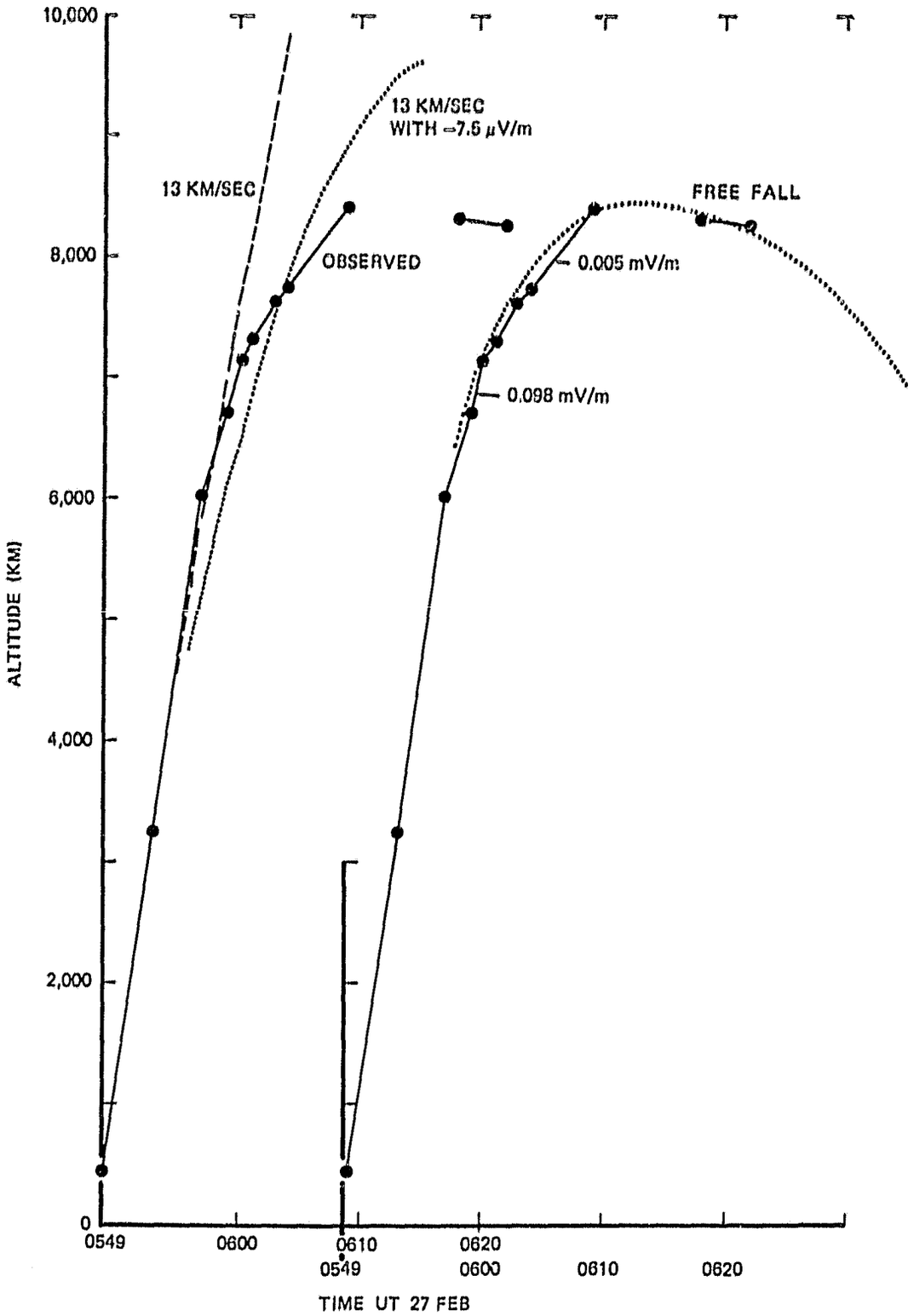


Figure 9. Barium tip altitude vs time. The initial velocity was observed at 13.0 km/sec. To fit the deceleration curve, a parallel electric field of -98 μV/m is applied for 1.6 minutes, then a field of -5 μV/m for 10 minutes.

# ARTIFICIAL AURORA CONJUGATE TO A ROCKET-BORNE ELECTRON ACCELERATOR

T. N. Davis[1], W. N. Hess[2], M. C. Trichel[3], E. M. Wescott[1],

T. J. Hallinan[1], H. C. Stenbaek-Nielsen[1], and E.J.R. Maier[4]

[1]Geophysical Institute
University of Alaska
Fairbanks, Alaska 99701

[2]NOAA Research Laboratories
Boulder, Colorado 80303

[3]NASA Johnson Space Center
Houston, Texas 77058

[4]NASA Goddard Space Flight Center
Greenbelt, Maryland 20771

Revised: December, 1979

Submitted to the Journal of Geophysical Research

# Artificial Aurora Conjugate to a Rocket-borne Electron Accelerator

T. N. Davis[1], W. N. Hess[2], M. C. Trichel[3], E. M. Wescott[1],
T. J. Hallinan[1], H. C. Stenbaek-Nielsen[1], and E.J.R. Maier[4]

[1]Geophysical Institute, University of Alaska, Fairbanks, Alaska 99701

[2]NOAA Research Laboratories, Boulder, Colorado 80303

[3]NASA Johnson Space Center, Houston, Texas 77058

[4]NASA Goddard Space Flight Center, Greenbelt, Maryland 20771

## ABSTRACT

An accelerator intended to send electron beams upward along an $L = 1.24$ magnetic field line was flown from a rocket launched from Kauai, Hawaii, on October 15, 1972. Though the intent was to produce several hundred observable auroral streaks in the southern hemisphere, imaging instruments operated there aboard jet aircraft detected only a single aurora. Produced by a 0.155 ampere beam of energy 22.8 keV, the aurora was of expected brightness, had diameter ($210 \pm 50$ m) somewhat larger than expected, and altitude (top: $116 \pm 2$ km; bottom: $92 \pm 2$ km) higher than expected.

## I. INTRODUCTION

The first rocket-borne electron accelerator to produce optically observed artificial aurora was flown from Wallops Island, Virginia in January, 1969 (Hess et al., 1971). Several raylike auroras were detected below the downward pointing accelerator, the auroras being produced by electron beams of energy 8.7 keV, current 490 mA and duration 1 sec (Davis et al., (1971)). Here we report on a follow-on experiment wherein

an artificial aurora was observed in the Southern Hemisphere conjugate to an upward-directed electron accelerator. The accelerator was flown on a rocket (NASA 12.18 NE) launched from the Pacific Missile Range Facility at Kauai, Hawaii, at 1500 October 15, 1972 (UT). This experiment, jointly sponsored by NASA and AEC, was one of several rocket experiments performed during Operation PICAPOSTE in October, 1972 (Peek and Joy, 1972; Wescott et al., 1974). Though during the course of this experiment more than 200 artificial auroras could have been produced in the atmosphere conjugate to or below the accelerator, only a single aurora was observed--in the conjugate hemisphere.

The long delay in publication of these results is due to several causes, not the least of which has been our inability to arrive at an internally consistent interpretation of data from instrumentation aboard the accelerator payload. Even yet, we lack full comprehension of what transpired during the experiment. Over the years, we have gained confidence that we (1) know the attitude of the electron accelerator during its flight, (2) have evolved quantitative information on the threshold required for an image orthicon television to detect a weak artificial aurora, and (3) have an accurate representation of the profile of the intensity of the artificial aurora as a function of altitude. These three advances have allowed us to evolve what we think is a reasonable partial interpretation of the results of this electron accelerator experiment. Some results presented here have been referred to in earlier papers by Wescott et al. (1972) and Wescott et al. (1974); also some were presented orally to the American Geophysical Union (Davis, 1973). Also, there is available a limited circulation report (Davis et al., 1979) giving additional details of the experiment.

## 2. INSTRUMENTATION

### 2.1 Payload and Vehicle Systems

#### 2.1.1 Electron Accelerator

The accelerator was built by Ion Physics Corporation in similar fashion to the one flown earlier at Wallops Island (Hess et al., 1971; Harrison, 1973). It consisted of a battery supply, high-voltage converters, a pulse programmer, a beam-current controller and six sealed electron guns as well as other circuitry and power supplies for operational and monitoring functions. The six electron guns were mounted on a 28 cm diameter circle on the front plate of the accelerator so as to point forward along the rocket thrust axis. These guns, of tetrode structure, had 0.8 $cm^2$ oxide cathodes. Protective ceramic envelopes equipped with anode caps permitted testing prior to flight; these envelopes were designed to be jettisoned at altitude by means of springs subsequent to the passage of high current through metallic breakseal bands.

The electro-mechanical programmer was designed to provide a 44-pulse sequence of beams of energy 5, 10 and 20 keV, current 200 or 500 mA and duration 0.01, 0.15, 1.0, 2.0 and 6.0 sec according to a predetermined schedule (Davis et al., 1979). Once initiated, this sequence would be repeated until payload reentry.

Associated with the accelerator package was a deployable collector screen, 26 m in diameter, as described earlier by Hess et al., (1971). Its purpose was to provide a large cross section for collection of ambient electrons for payload neutralization. Telemetry outputs were provided to monitor the accelerator voltage, beam current, total collector current, four currents from different portions of the front and rear of

the collector assembly and a variety of other operational parameters such as battery voltages, temperatures, pressures and event occurrences.

2.1.2 Rocket and Attitude Control Systems

The payload was flown on a Strypi 4 two-stage solid propellent rocket. The second stage consisted of a spherical motor inside a cylindrical section 0.8 m in length and diameter, into which the payload partially penetrated. Following burn-out of the second stage motor, the payload was separated from that stage. Contained within the cylindrical portion of the 0.8-m diameter payload section were a three-axis attitude control system, a 2-axis fluxgate for attitude monitoring, and telemetry components. Most of the accelerator package was forward of this section in the payload nose cone. Telemetry antennas, beacon antennas and a despin yo-yo were mounted in the cylindrical portion of the payload, well behind the plane in which the large collector screen was to be deployed. With the exception of sealed battery boxes and the accelerator, pressurized under 2 atm of $SF_6$, the entire payload volume was evacuated before launch to reduce the probability of high-voltage breakdowns and gas poisoning of the accelerator's gun cathodes.

2.1.3 Additional Instrumentation

Mounted on the front deck near the accelerator's guns was an electron spectrometer containing several channeltron detectors from which no useful data were obtained. Also mounted on the forward deck of the accelerator was a multigrid retarding potential analyzer (RPA) similar to that described by Serbu and Maier (1966) with its retarding potential designed to sweep over the range 0 to 500 V approximately once each second. An identical RPA was placed on the rear of the

payload. Similarly mounted to view backwards was a third RPA with a fixed potential switched between -3 V and -8 V every 2 sec.

A radio receiver system sensitive to waves in the range 20 Hz to 10 MHz, provided by D. G. Cartwright of the University of Minnesota, was mounted on the second stage of the Strypi rocket. So mounted, this receiver system was isolated from the accelerator payload after separation, but its overall flight trajectory was similar.

2.2 Ground-Based and Aircraft Systems

During Operation PICAPOSTE, of which this experiment was a part, numerous instruments were deployed in the Hawaiian Islands, on two NC-135 aircraft and elsewhere. Here we describe only those instruments particularly suited for observations of artificial aurora produced by the electron accelerator.

One image orthicon television camera identical to those used earlier during the 1969 experiment (Davis et al., 1971) and a similar system were operated at an observatory on Mt. Haleakala, Maui, Hawaii. The cameras at this location viewed the sub-trajectory 100-km level where auroras produced by backscattered beams or downward-directed beams should appear. Being approximately 550 km eastward of the sub-trajectory path, this location provided a near-normal viewing aspect to the direction of the magnetic field at a low elevation angle, near 10°.

The region in the Southern Hemisphere where auroras were expected to appear lies over water at approximately 22° S, 170° W, a location south of Niue Island and east of Tonga. Consequently, the primary observations of artificial auroras were made with electronic imager cameras mounted in two NC-135 jet aircraft positioned as shown in

Fig 1

Figure 1. In each aircraft was an image orthicon camera identical to that at Haleakala. These cameras were on manually-steered mounts and were arranged to view through windows on the right-hand side of each aircraft. Additional television cameras of similar or lower sensitivity were operated on semi-automatically controlled tracking benches, also on the right-hand side of the aircraft. These latter cameras had fields of view near 16° x 20°, somewhat larger than the 12° x 16° field of view of the image orthicons mentioned above.

## 3. CONDUCT OF THE EXPERIMENT; FLIGHT PERFORMANCE

### 3.1 Geophysical Environment

The rocket was launched at 1500 October 15, 1972, a time of minor magnetic disturbance. The preceding 3-hour range index Kp was 2, and the following 1+ (Lincoln, 1973). The AE index (Allen et al., 1975) showed that a minor substorm (Max AE $\approx$ 300 $\gamma$) had started a few minutes before liftoff. Optical observing conditions at Haleakala and the two aircraft locations were excellent.

### 3.2 Rocket and Attitude Control Performance

The rocket system achieved near-nominal performance, lifting the payload nearly along the predicted trajectory with apogee 398 km at T + 341.8 sec, 150 km downrange along azimuth 209° (see the altitude versus time profile in Figure 2). Following burn-out of the second stage rocket at T + 95 sec, the payload was separated from it (at T + 105 sec) and despun (at T + 107 sec). The attitude control system (ACS) was initiated at T + 116 sec and operated until T + 148 sec, after which time it was never again activated. This gyro-controlled system was supposed to reorient the payload by approximately 60° so as to point its

Fig 2

longitudinal axis upward along the direction of the local magnetic field. However, the telemetered monitor of the gyro control showed that erratic gyro behavior occurred essentially from the time of launch. The apparent gyro platform attitude drifted more than 100° relative to the magnetic field vector $\vec{B}$ during the first 100 sec of flight. Consequently, the reorienting maneuver was improperly performed and brought the payload axis to only within 40° of the direction of $\vec{B}$, where the attitude remained stable until T + 160 sec. The large collector foil was deployed at T + 144 sec.

Fig. 3

As shown in Figure 3, the payload underwent a violent change in attitude commencing at T + 160 sec. Since at this instant there was abrupt failure of the radio receiver system mounted on the second stage motor, it is conjectured that the previously separated payload and the second stage motor collided at T + 160 sec. The plot of attitude in Figure 3 shows irregular variation in payload attitude until after T + 220 sec. Thereafter the attitude, relative to $\vec{B}$, oscillates in a more regular fashion between one extreme where the accelerator was directed down along $\vec{B}$ to another where the accelerator pointed upward to within 45° to 60° of $\vec{B}$. Thus, according to the onboard fluxgate magnetometer data, the accelerator was never pointed so as to eject electrons upward with pitch angles less than 45°.

### 3.3 Accelerator Performance

The telemetered monitoring data show that the various functions required to initiate the accelerator operation occurred as scheduled. The programmer initiated the first pulse A1 at T + 192 sec, the accelerator being at altitude 300 km and pointed downward along $\vec{B}$ (opposite to the

planned direction). The temporal performance of the programmer thereafter was without flaw until reentry; the 44-pulse sequences A,B,C,D, and a portion of sequence E were completed as scheduled (see Fig. 2).

Monitors of the accelerator voltage and current and of the current from the collector to the accelerator showed erratic behavior during the first 20 pulses (A1 to A20). Sustained arcing appears to have occurred during the first few pulses, and intermittent arcing occurred thereafter. During pulses A21 through B10 (T + 240 sec to T + 315 sec) there appears to have been no arcing and no accelerator output, all current monitors showing zero current.

Beginning with pulse B11, the monitors of beam and collector current showed these two quantities rising monotonically in unison through pulse B25 (T + 347 sec). Throughout this interval the pulse program called for nominal accelerator voltage 20 kV; the actual value during each pulse was 22.8 keV. Although the beam current should have been either 200 mA or 500 mA throughout the program the maximum current achieved up to pulse B25 was approximately 100 mA. Pulses B26 through B31 had nominal voltage 10 kV, but the actual value was 14 kV, according to the voltage monitor. The beam current during pulses B26 to B31 ranged from 90 to 102 mA, apparently independent of whether the nominal current for a particular pulse was 200 mA or 500 mA.

Pulses B32 through B37 all were nominally 20 kV, 200 mA or 500 mA, with actual voltage and current being 22.8 kV, and 134 mA, respectively. Nominally 5 kV and 200 or 500 mA pulses, pulses B38 through B43 actually were 5.2 kV with current 90 to 102 mA.

Pulse B44, the only one producing an observed aurora and therefore the only one for which there is definite proof of the escape of the

electron beam, was of voltage 22.8 kV and current 155 mA. Pulses C1, C2, C3 and C4, following within 10 sec of pulse B44, were identical to pulse B44 in voltage and nearly identical in current (144 to 155 mA) according to the monitor data. Yet these pulses did not produce aurora. Except for pulse C1, of only 0.01-sec duration, the aircraft-borne instrumentation would have detected any aurora produced from these pulses.

Throughout the remainder of the flight, the monitors of accelerator voltage, accelerator beam current and total collector current showed an unvarying pattern of behavior. All nominally 10-kV pulses were of actual voltage 13.6 to 14.0 kV and current 113 to 130 mA. Similarly, the nominally 5-kV pulses were of actual voltage 4.8 to 5.2 kV and current 90 mA. The actual beam currents appeared to be independent of whether the programmed nominal current was 200 mA or 500 mA. In all cases, the apparent total collector and beam currents were identical to within 10%, the range of measurement error.

On the basis of the outputs of the monitors of payload attitude, payload functions and accelerator performance, we conclude the following sequence of events. It appears that there was malfunction of the gyro control of the attitude control system since the monitor of gyro output showed impossible readings early in the flight. For that or other reasons, the payload was not oriented to point upward along $\vec{B}$ prior to deployment of the collector screen at T + 143 sec. Simultaneous abrupt tumbling of the payload and failure of electronic systems on the separated second stage suggest that these two bodies collided at T + 160 sec. Early in the programmed pulsing of the accelerator, sustained arcing followed by intermittent arcing suggests an abnormal gaseous atmosphere

in the vicinity of the guns, perhaps from the attitude control system. Zero accelerator output during the interval T + 240 sec to T + 315 sec, followed by a slow increase in gun output from T + 315 sec to T + 347 sec, suggests the possibility that the gun cathodes were poisoned during the arcing and that they later partially recovered.

## 4. RESULTS

### 4.1 Results from Onboard Detectors

Owing to the failure of the radio-frequency receiver system prior to initiation of the accelerator sequencing, no results on rf emissions were obtained. Of the onboard instruments, only the retarding potential analyzers appear to have performed satisfactorily, but no detailed analysis of the data has been performed.

### 4.2 Results from Ground-based and Aircraft-borne Imagers

The image orthicon operated on Mt. Haleakala, Maui, Hawaii, was oriented properly to view the 100-km level of the sub-trajectory throughout the rocket's flight. Nevertheless, improved knowledge gained in recent years (Davis et al., 1975; Hallinan et al., 1978) dictates that the imager on Mt. Haleakala could not have detected any artificial auroras produced by backscatter or direct injection below the accelerator. Observations during subsequent electron beam experiments have allowed us to calculate the beam power needed to observe the artificial auroral streak as a function of magnitude of the faintest stars visible in the television images. Given the viewing conditions and observational parameters at Mt. Haleakala, it is evident that the electron beam energy was insufficient for detection. Thus it is quite possible that the electron accelerator generated auroras in the Northern Hemisphere but that these went unobserved.

At the times shown on Figure 3, one or more of the imaging cameras on the two jet aircraft were properly oriented to detect artificial auroras produced in the atmosphere of the Southern Hemisphere, conjugate to the location of the accelerator. However, not until near the end of the first (A) sequence was the accelerator oriented to within the required 63° of the magnetic field direction that would permit upward ejected electrons to reach the atmosphere of the Southern Hemisphere. This requirement is based upon evaluation of an equation (Equation 2.58) given by Roederer (1970) for the L-value (L=1.24) pertinent to the experiment; it being assumed that the electrons are moving adiabatically in a dipole magnetic field. At this L-value the equatorial loss cone has half-aperture 40°; to have equatorial pitch angles within the cone the electrons must be ejected from the accelerator with pitch angles $\leq 63°$.

Even though Figure 3 shows an interval near T + 260 sec when both the accelerator and one or more aircraft imagers were oriented to allow observed auroras in the Southern Hemisphere, the accelerator monitors indicate little output during this interval. Figure 3 shows that the next possibility of producing and observing an aurora in the Southern Hemisphere is the 20-sec interval commencing near T + 378 sec. The only observed aurora, that from accelerator pulse B44 was observed during this time. Again, near T + 556, there is a brief interval when auroras could have been produced and might possibly have been observed in the Southern Hemisphere.

Fig. 4

The aurora produced by pulse B44 (Figure 4) had brightness approximately equal to that of an IBC II aurora and was easily detected by two imagers on Aircraft 369, see Figure 1, but the imagers on Aircraft 370

were not oriented properly to detect the aurora. The lack of observation from two widely separated locations prevented direct triangulation of the position of the artificial aurora. However, if the ray-like artificial aurora is oriented exactly along the direction of the magnetic field, it is possible to determine uniquely the aurora's position in space. The expectation that such auroras are field-aligned is verified by the results obtained from the previous experiment at Wallops Island (Davis et al., 1971). In addition to the assumption of the aurora's being field-aligned, this single-station method requires an adequate model of the geomagnetic field.

Prior to this experiment, calculations by G. D. Mead and shaped-charge barium releases (Wescott et al., 1972) had already shown that the various available models of the magnetic field were inaccurate in this part of the world, mainly because the models diverged when updated to the epoch of the experiment. Evidently the culprit is the method of adjusting the models for secular variation rather than the time-independent versions of the models themselves.

Of the models available, three gave closely agreeing results. These models were POGO 8/69 epoch 1964.3 (Cain and Sweeney, 1970), POGO 10/68 epoch 1965.8 (Cain and Langel, 1971) and OGO 246 epoch 1965.3 (R. Langel, private communication, 1972; see also Wescott et al., 1974). The three models gave the observed aurora the same areal location to within 3 km and agreed closely in giving the top and bottom altitudes of the aurora, 116 $\pm$ 2 km and 92 $\pm$ 2 km, respectively. The altitude of maximum brightness of the aurora was found to be 102.5 $\pm$ 2 km.

Two different techniques have been used to obtain plots of luminosity versus altitude along the artificial auroral ray, both techniques giving similar results. One method, the one used to obtain results presented in Figures 5-9, involved photography of auroral images displayed on a TV screen to obtain negatives that could be scanned with a densitometer. The density produced in the film is related to the intensity of the light, the exposure time, the film characteristics and development. The relationship can be formalized by $I \alpha 10^{\frac{d}{\gamma}}$, where I is the intensity, d is the film density and $\gamma$ is the slope of the linear portion of the curve of density versus log exposure for the film. In the data analysis, $\gamma$ of the film was carefully controlled and measured by use of calibrated density step wedges. Intensity is arbitrary, however, since the constant of proportionality is unknown. The equivalent $\gamma$ of the TV camera electronics, tape recorder and TV monitor system was not calibrated specifically. However, later tests have shown that $\gamma$ is close to 1. In subsequent computations of the artificial auroral intensity (to arbitrary scale) an overall system $\gamma = 1$ was assumed.

FIG. 5
FIG. 6
FIG. 7
FIG. 8
FIG. 9

Profiles of intensity versus altitude each 0.1 sec of the 1-sec lifetime of the auroral ray are shown in Figure 5, where 3-point running averages of the sampled points are plotted as solid curves. Variation in the overall intensity with time is evident in Figure 5 but is shown better by the plot of peak intensity versus time given in Figure 6. A trend toward increasing altitude of the position of peak luminosity is evident in the plot of Figure 7. The increase in peak intensity during the first 0.3 sec probably is due to to the increase in the OI 5577 component of the observed emission in consequence of the parent 'S state having about an 0.7-sec lifetime. An increasing 5577 component might

also explain the trend toward increasing altitude shown by Figure 7; alternately the increase in altitude could be due to a softening of the causative particle spectrum during the lifetime of the aurora.

That the profile of intensity versus height of the artificial aurora differs radically from that of natural rayed aurora is shown in Fig. 8. There the same technique has been applied to obtain profiles of weak and bright auroral rays recorded in the auroral zone by identical imagers viewing at similar aspect to the magnetic field direction. Comparison of the curves in Figure 8 implies that the particle beam arriving in the atmosphere to cause the artificial aurora is much more monoenergetic than those causing the natural auroral rays.

Following Berger et al. (1970), profiles of energy deposition versus altitude have been calculated for various electron energies, taking into account the inclination of the magnetic field and using a model of atmospheric density appropriate to the location of the artificial aurora. On these profiles, shown in Fig. 9, is superposed a plot of the measured intensity versus altitude profile of the artificial aurora.

Measurement of the diameter of the artificial auroral ray produced by Pulse B44 gave a value of 210 $\pm$ 50 m, corrected for an inherent widening of the image of the ray by the characteristics of the TV imager and motion of the accelerator transverse to the magnetic field. This diameter is larger than the 130 $\pm$ 50 m diameter measured in the experiment at Wallops Island (Davis et al, 1971) and more recently at Poker Flat, Alaska, by Hallinan et al. (1978) where diameters ranging from 34 to 182 m were observed. Both cited experiments involved downward, rather than upward, ejection of electrons at voltages ranging from 8 keV to 40 keV.

The artificial aurora was detected in the conjugate region at 15:06:22.06 $\pm$ 0.025 sec, and the beam was initiated at 15:06:21.86 $\pm$ 0.00 sec. Relative clock errors between the launch site and the aircraft were stated by cognizant personnel to be less than 0.01 sec. Assuming no unknown clock error, the measured travel time of the electron beam was 0.200 $\pm$ 0.025 sec.

## 5. DISCUSSION AND CONCLUSIONS

The probable collision of the payload and the booster rocket at T + 160 sec, signaled by abrupt failure of instrumentation on the booster rocket and abrupt tumbling of the payload, likely was responsible for subsequent unplanned events during the course of the experiment. The violent tumbling of the payload indicated by the plot in Figure 3 must surely have caused differential motion between the main payload and 26-m diameter collector screen. Such differential motion could explain the damping of the payload's oscillatory motion prior to T + $\sim$220 sec. Figure 3 indicates, thereafter, that fairly regular motion with a period near 70 sec ensued. It seems entirely possible that the collector wrapped up around the payload and may have trapped gases from the attitude control system, leading to poisoning of the electron guns during their early operation. Though the guns apparently partially recovered, never was more than a third of the planned output achieved.

Failure to detect any artificial auroras in the Southern Hemisphere prior to the end of the second (B) pulsing sequence of the accelerator seems to be adequately explained by the combination of improper payload attitude and accelerator cathode poisoning. Similarly, the failure to detect auroras after T + 400 sec can be attributed to a combination of improper payload attitude and improper aiming of the aircraft-based TV

cameras. A possible exception occurred for a few seconds near T + 556 sec; Figure 3 shows that payload attitude and camera aiming were marginally such that auroras might have been produced and detected.

We still have no truly acceptable explanation of why accelerator pulses C2, C3 and perhaps C4 did not produce observable auroras in the southern hemisphere. During pulse C4 the payload attitude swung through the limiting pitch angle (63°) beyond which electrons could not penetrate to the Southern Hemisphere's atmosphere before being magnetically mirrored; otherwise the payload attitude was in the acceptable range.

It is possible to compare the observed transit time of the electron beam to the southern hemisphere, 0.20 $\pm$ 0.025 sec with the bounce period using a formula given by Roederer (1970): his Equation 2.60

$$T_b = \frac{4\ R_e}{c}\ L\ f(\alpha_o)\ \beta^{-1} \qquad (1)$$

where $R_e$ is the radius of the earth, c is the velocity of light, L is the McIllwain parameter, $\beta$ is the speed of the electron divided by the speed of light and $f(\alpha_o)$ is a function of the equatorial pitch angle $\alpha_o$. Pulse B44, being launched from near altitude 400 km at pitch angle 48° would have achieved equatorial pitch angle $\alpha_o$ = 32° on the L = 1.24 field on which it was traveling. The accelerator voltage of 22.8 kev corresponds to a relativistic beam speed $\beta$ = 0.2887. Values of the function $f(\alpha_o)$ are given in Table 1 of the book by Schultz and Lanzerotti (1974). The value of $f(\alpha_o = 32°)$ = 0.9773. Consequently Equation 1 gives a value of $T_b$ = 0.3568 when the appropriate parameters are inserted. The half-bounce period is then 0.1784 sec, in close agreement with the observed travel time.

There is no indication from the brightness of the observed aurora that the electron beam lost kinetic energy in transit to the Southern Hemisphere. The aurora's apparent brightness of approximately IBC II seen 33° off-axis results from a viewing pathlength of 385 m through the 210-meter diameter aurora. A height integration of the observed profile shown in Figure 9 indicates that it is equivalent to a column 8.6 km long with volume emission equal to that at the altitude of maximum brightness. Hence, the aurora would have had a surface brightness 22 times greater had it been viewed parallel to its axis, a brightness roughly twice that of an IBC III aurora. Assuming 0.6 ergs $cm^{-2}$ $sec^{-1}$ energy deposition in an IBC I aurora, the energy deposition in the artificial aurora is approximately 120 ergs $cm^{-2}$ $sec^{-1}$. Then, the total deposition in the beam of 210-m diameter is roughly $4 \times 10^{10}$ ergs $sec^{-1}$.

Pulse B44 that produced this aurora had energy 22.8 keV and current 155 mA. Hence the rate of energy output was $3.4 \times 10^{10}$ ergs $sec^{-1}$. The excellent agreement between accelerator output and energy deposition is little more than accidental since the estimate of auroral brightness may be in error by several hundred percent. Nevertheless, there is no suggestion in these calculations of loss of kinetic energy from the beam prior to its arrival in the atmosphere of the Southern Hemisphere.

## ACKNOWLEDGMENTS

Major contributions to the performance of this experiment were made by personnel of Los Alamos Scientific Laboratory working under the direction of Dr. H. Milton Peek and Dr. Robert A. Jeffries and personnel of Sandia Laboratories working under the direction of H. E. Hanson. The work at the Geophysical Institute was supported by the National Aeronautics and Space Administration through grants NGR 02-001-087 and NSG-6014 and contract NAS 9-11815 to the Geophysical Institute.

## REFERENCES


Allen, J. H., Auroral electrojet magnetic activity indices AE(11) for 1972, ADC-2 Report, UAG-45, NOAA Environmental Data Service, Boulder, Colorado, 1975.

Davis, T. N., C. S. Deehr, T. J. Hallinan, and E. M. Wescott, AMPS definition study on optical band imager and photometer system (OBIPS), Final Rept., NASA Contract NAS9-14645, Geophysical Institute, Univ. of Alaska, Fairbanks, Alaska, 184 pp., Sept., 1975.

Davis, T. N., T. J. Hallinan, G. D. Mead, J. M. Mead, M. C. Trichel and W. N. Hess, Artificial aurora experiment: Ground-based optical observations, J. Geophys. Res., 76, 6082, 1971.

Davis, T. N., W. N. Hess, M. C. Trichel, E. M. Wescott, T. J. Hallinan, H. C. Stenbaek-Nielsen, and E. J. R. Maier, Artificial Aurora conjugate to a rocket-borne electron accelerator, Rept. UAG-R270, Geophysical Institute, Fairbanks, Alaska, 99701, Dec., 1979.

Hallinan, T. J., H. C. Stenbaek-Nielsen, and J. R. Winckler, The Echo 4 electron beam experiment: television observation of artificial auroral streaks indicating strong beam interactions in the high-latitude magnetosphere, J. Geophys. Res., 83, 3263-3272, 1978.

Harrison, R., 20 Kilovolt rocket-borne electron accelerator, Final Report on Contract NAS9-10399, Ion Physics Corp., Burlington, Mass., 1973.

Hess, W. N., M. C. Trichel, T. N. Davis, W. C. Beggs, G. E. Kraft, E. Stassinopoulous and E.J.R. Maier, Artificial aurora experiment: Experiment and principal results, J. Geophys. Res. 76, 6067, 1971.

Lincoln, J. V., Geomagnetic and solar data, J. Geophys. Res., 78, 780, 1973.

Peek, H. M. and K. N. Joy, PICAPOSTE Operations Plan, Los Alamos Scientific Laboratory, Los Alamos, N.M., October, 1972.

Roederer, J. G., Dynamics of Geomagnetically Trapped Radiation, Springer-Verlag, New York, 1970.

Schulz, M. and L. J. Lanzerotti, Particle Diffusion in the Radiation Belts, Springer-Verlag, New York, 1974.

Serbu, G. P., and E.J.R. Maier, Low-energy electrons measured on IMPZ, J. Geophys. Res., 71, 3755-3766, 1966.

Wescott, E. M., E. P. Rieger, H. C. Stenbaek-Nielsen, T. N. Davis, H. M. Peek and P. J. Bottoms, L = 1.24 Conjugate magnetic field line tracing experiments with barium shaped charges, J. Geophys. Res., 79, 159, 1974.

## Figure Titles

| Fig. No. | Title |
|---|---|
| 1 | Location of aircraft carrying imaging systems and the expected locus of the auroral streaks, at the 100-km level. The aircraft were held in oval flight patterns until the rocket was launched. |
| 2 | Altitude of the accelerator payload as a function of time from liftoff and times when each pulsing sequence of the electron accelerator was begun. |
| 3 | Attitude of the electron accelerator relative to a direction antiparallel to $\vec{B}$. The filled-in portions of the curve indicate the intervals when the pitch angle was low enough to allow electrons to penetrate the atmosphere of the Southern Hemisphere. Solid bars indicate intervals when at least one TV imager on the aircraft was aimed properly to see auroras, if generated. The overlapping dotted regions show when auroras would have been observed if generated. |
| 4 | At right, TV image obtained aboard aircraft 369 showing the artificial aurora produced by electron pulse B44. At left, shown for comparison is an artificial aurora produced in the 1969 Wallops experiment. The different appearance of the two auroras is largely due to the one at left being viewed more nearly perpendicular to the direction of the magnetic field. |

5 Height versus intensity profiles every 0.1 sec during the lifetime of the aurora resulting from pulse B44.

6 The peak intensity of the artificial aurora as a function of time during the 1-sec lifetime of the electron beam pulse.

7 Altitude of the position of peak luminosity of the artificial aurora versus time during the lifetime of the pulse.

8 Height versus luminosity profiles of the artificial aurora from pulse B44 together with profiles of a weak and a bright natural aurora obtained by the same technique and with comparable aspect angle relative to the direction of the geomagnetic field.

9 Profiles of energy deposition calculated for monoenergetic electron beams (solid lines) and a normalized plot of observed luminosity of the aurora resulting from pulse B44.

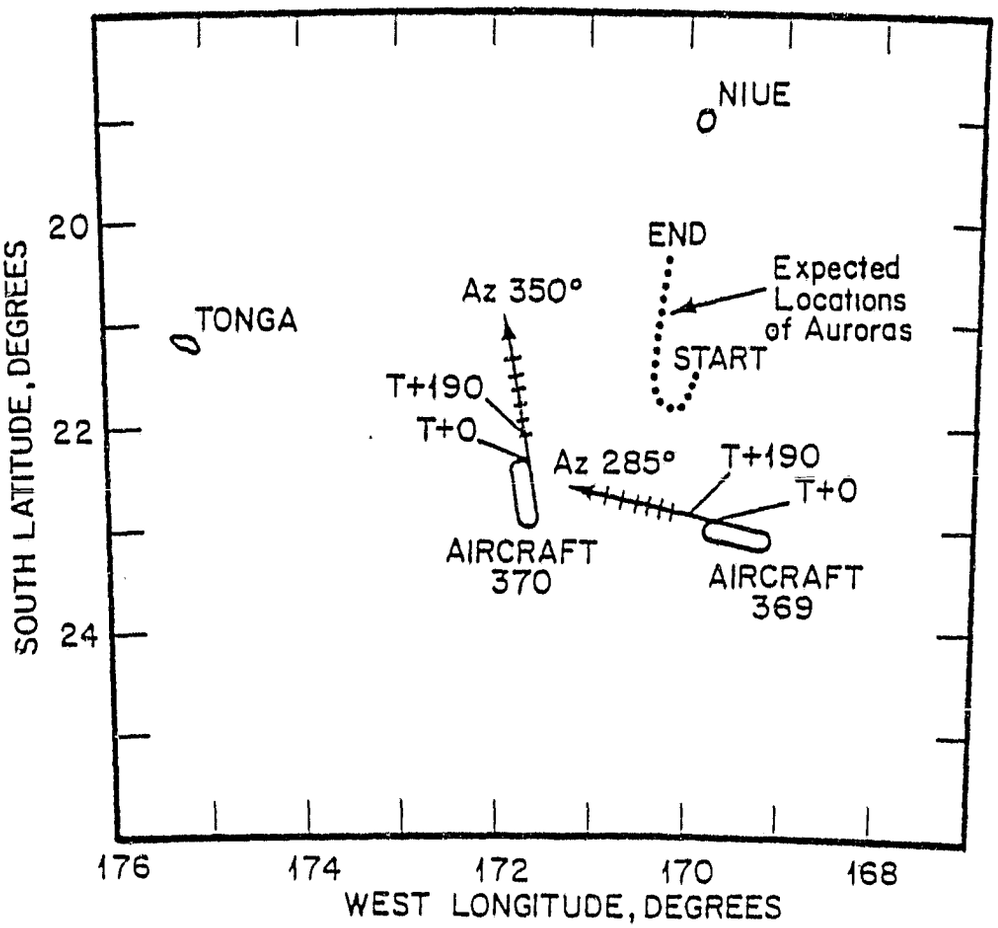


1 Location of aircraft carrying imaging systems and the expected locus of the auroral streaks, at the 100-km level. The aircraft were held in oval flight patterns until the rocket was launched.

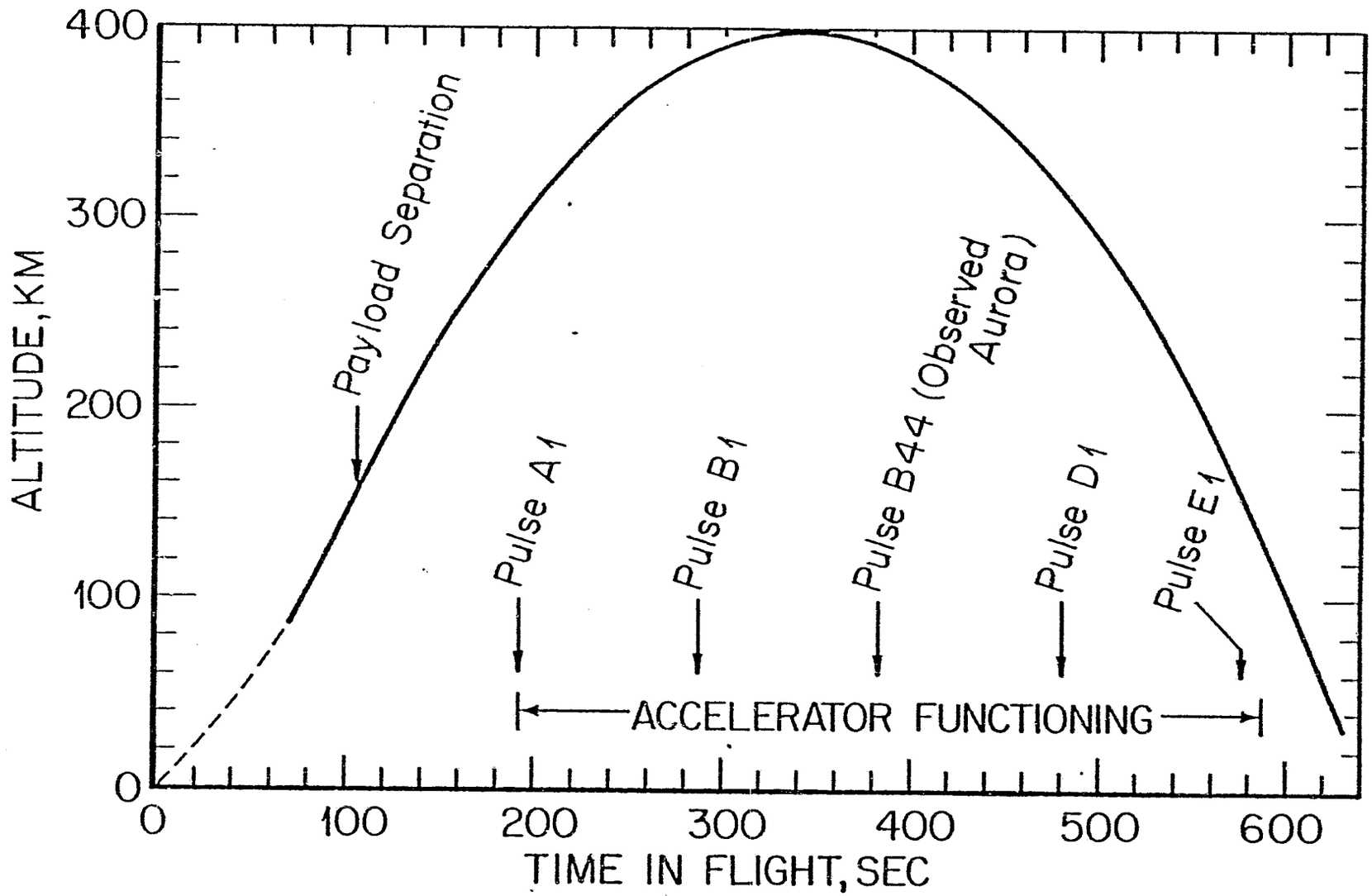


2 Altitude of the accelerator payload as a function of time from liftoff and times when each pulsing sequence of the electron accelerator was begun.

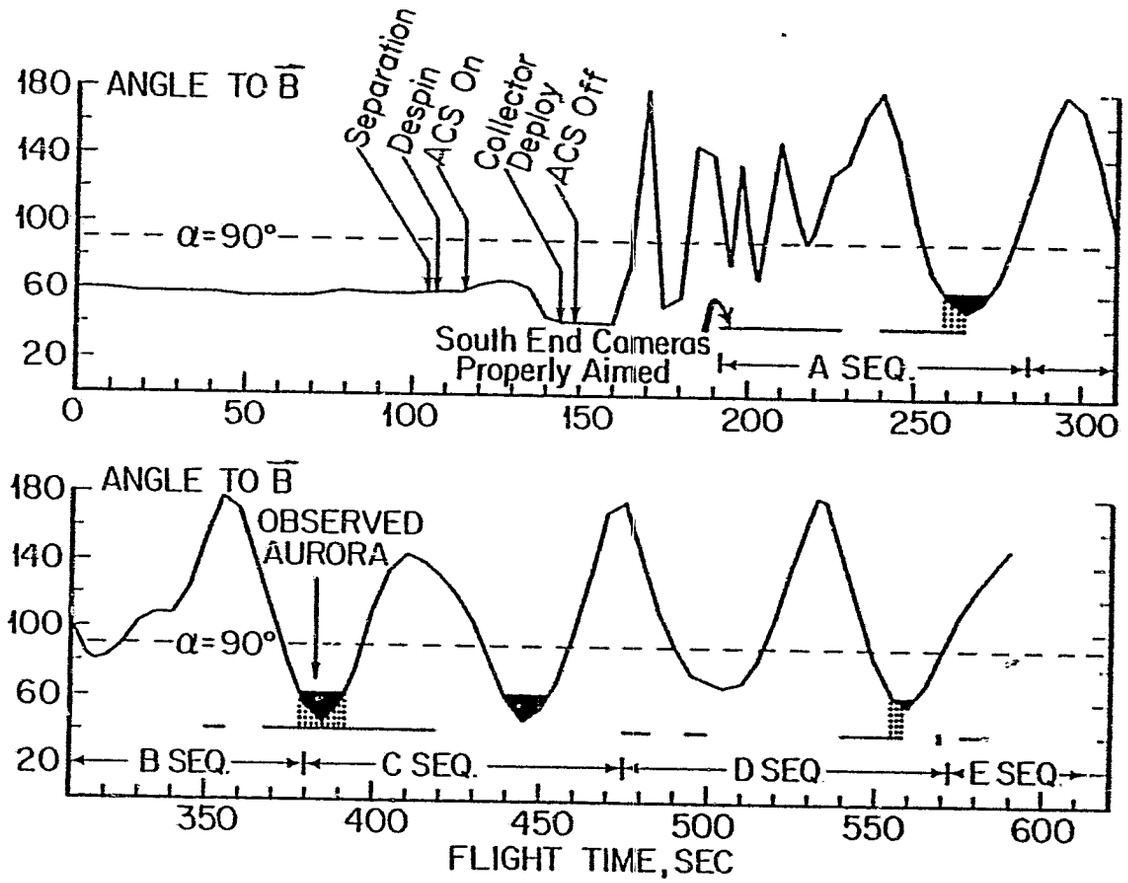


3 Attitude of the electron accelerator relative to a direction antiparallel to $\vec{B}$. The filled-in portions of the curve indicate the intervals when the pitch angle was low enough to allow electrons to penetrate the atmosphere of the Southern Hemisphere. Solid bars indicate intervals when at least one TV imager on the aircraft was aimed properly to see auroras, if generated. The overlapping dotted regions show when auroras would have been observed if generated.

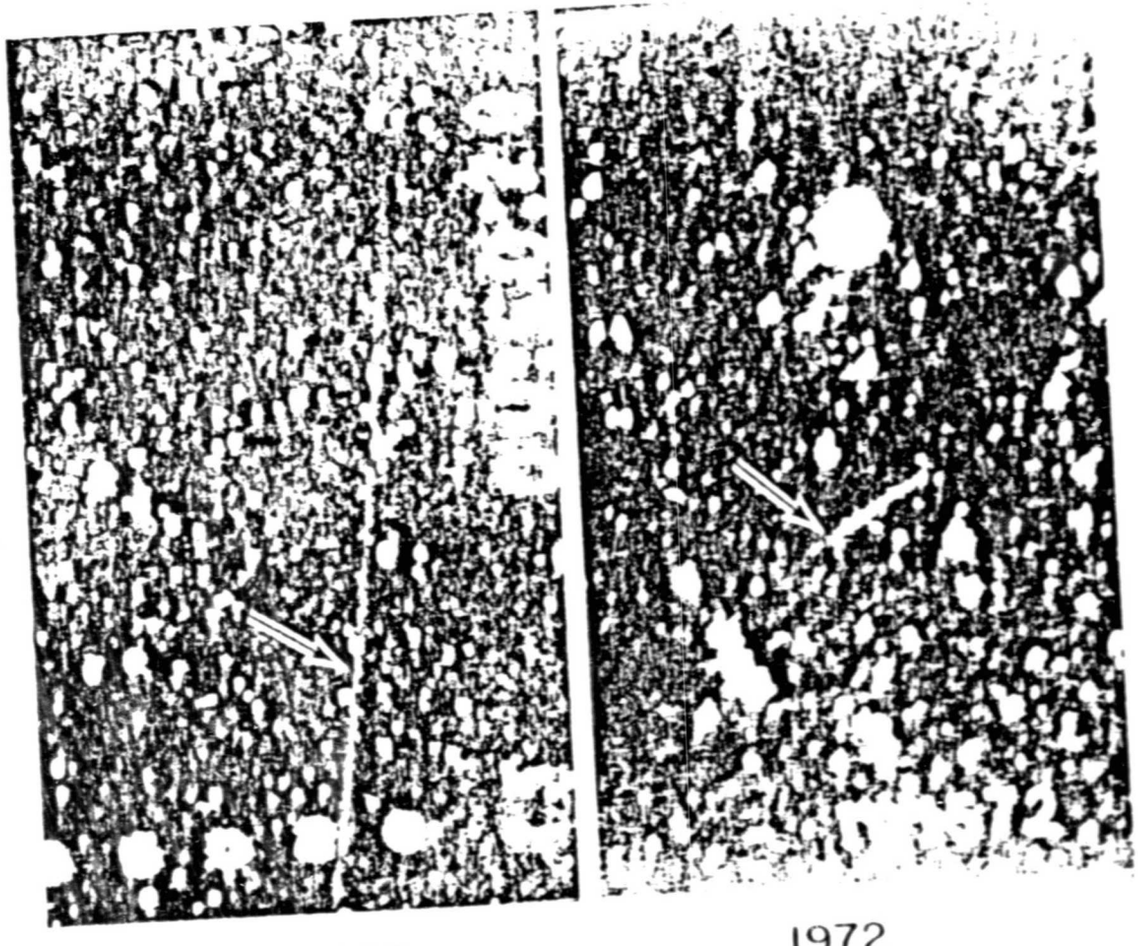

1969 1972

41

At right, TV image obtained aboard aircraft 369 showing the artificial aurora produced by electron pulse B44. At left, shown for comparison is an artificial aurora produced in the 1969 Wallops experiment. The different appearance of the two auroras is largely due to the one at left being viewed more nearly perpendicular to the direction of the magnetic field.

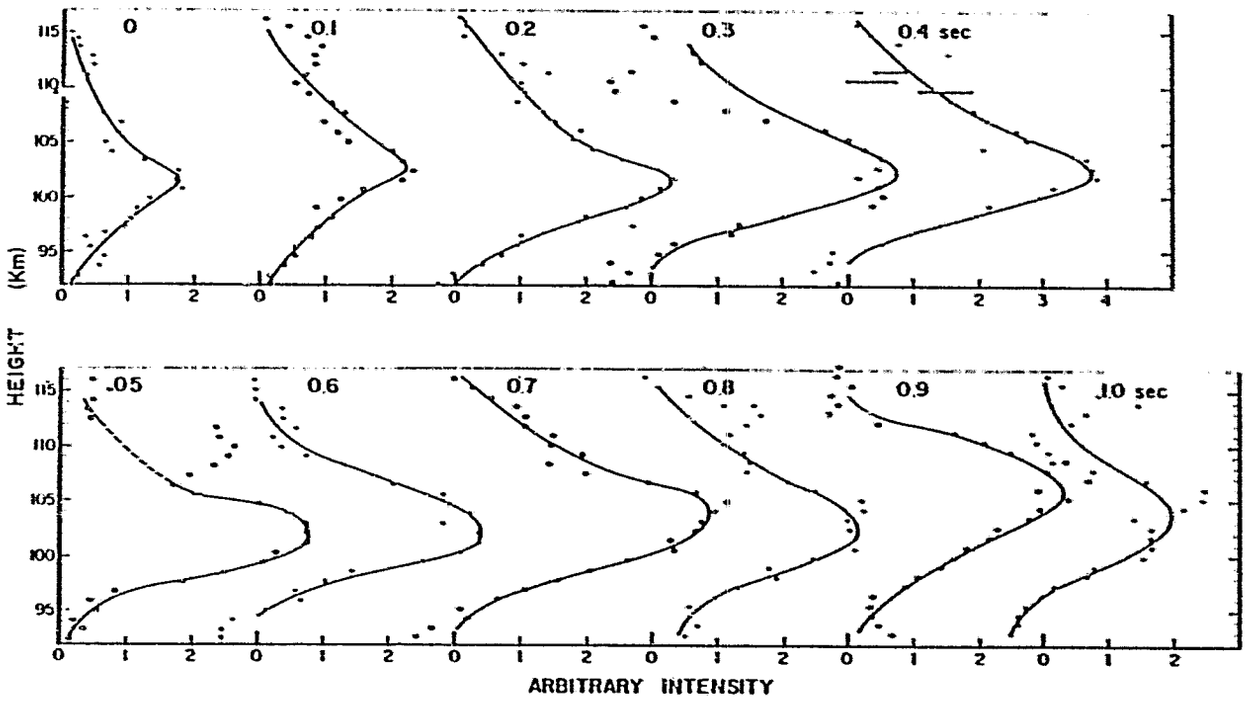


5

Height versus intensity profiles every 0.1 sec during the lifetime of the aurora resulting from pulse 844.

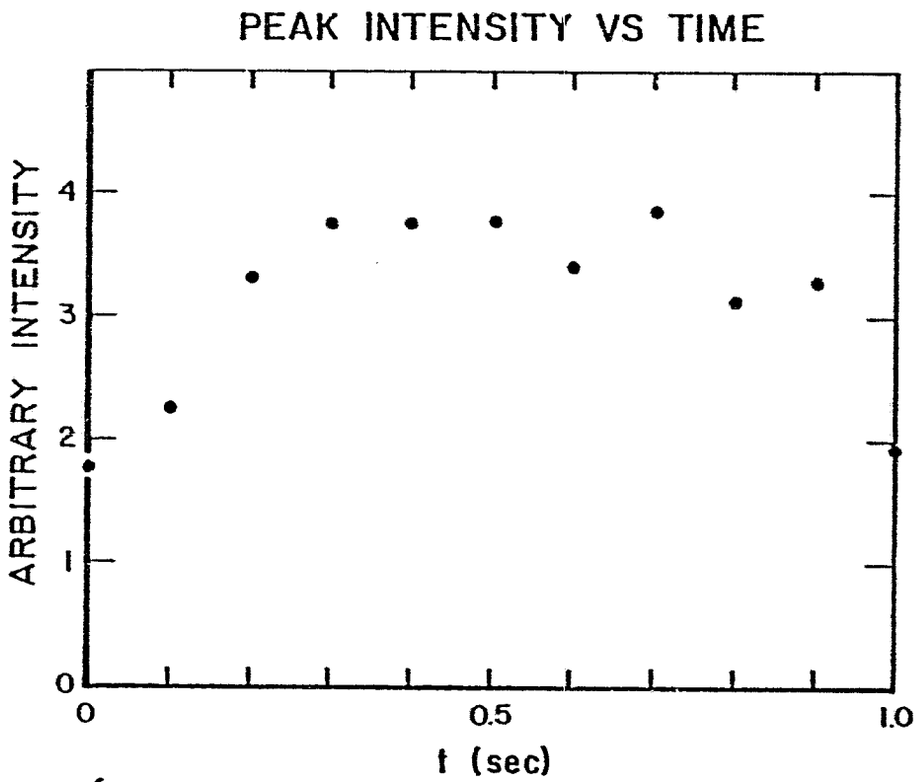


6

The peak intensity of the artificial aurora as a function of time during the 1-sec lifetime of the electron beam pulse.

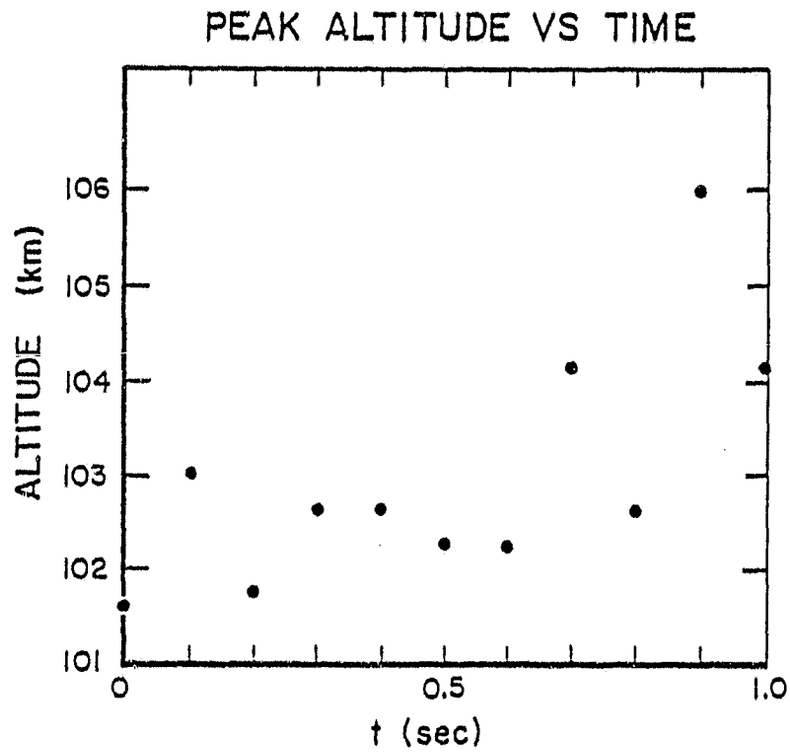


7

Altitude of the position of peak luminosity of the artificial aurora versus time during the lifetime of the pulse.

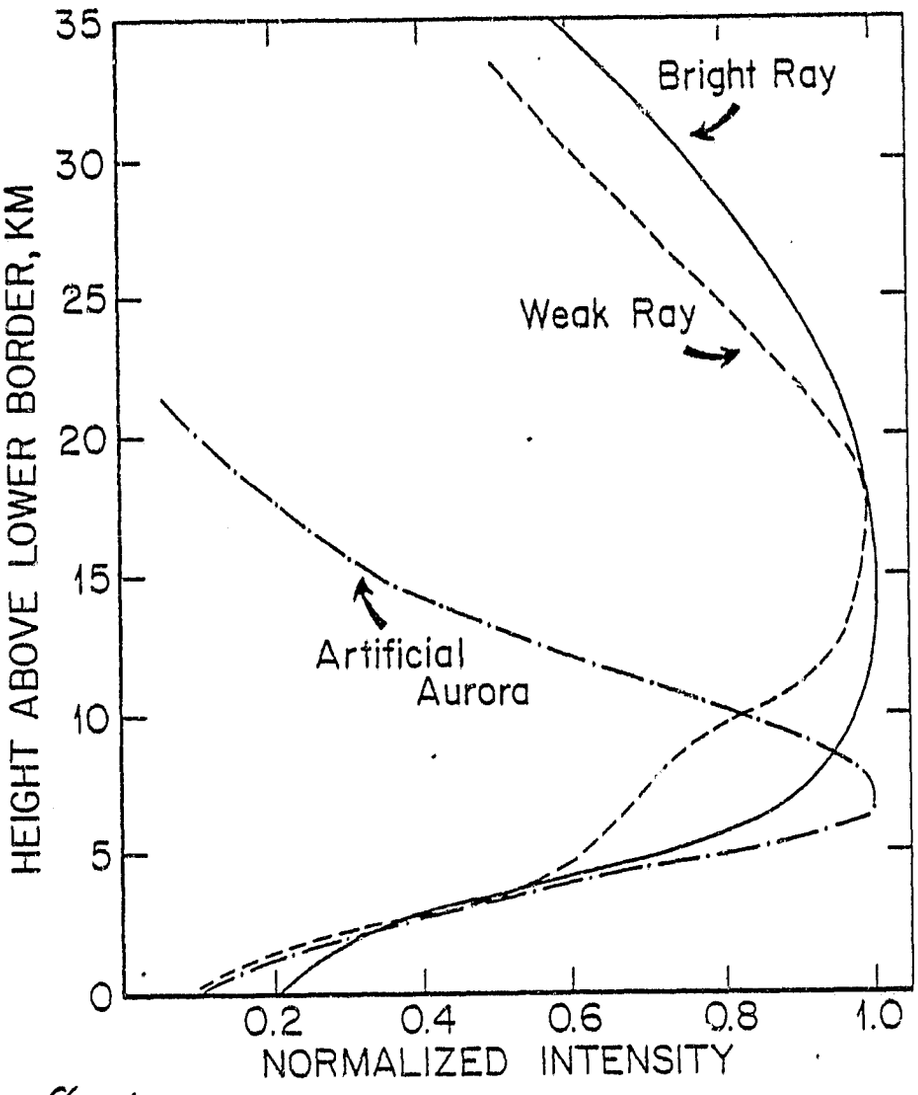


8

Height versus luminosity profiles of the artificial aurora from pulse B44 together with profiles of a weak and a bright natural aurora obtained by the same technique and with comparable aspect angle relative to the direction of the geomagnetic field.

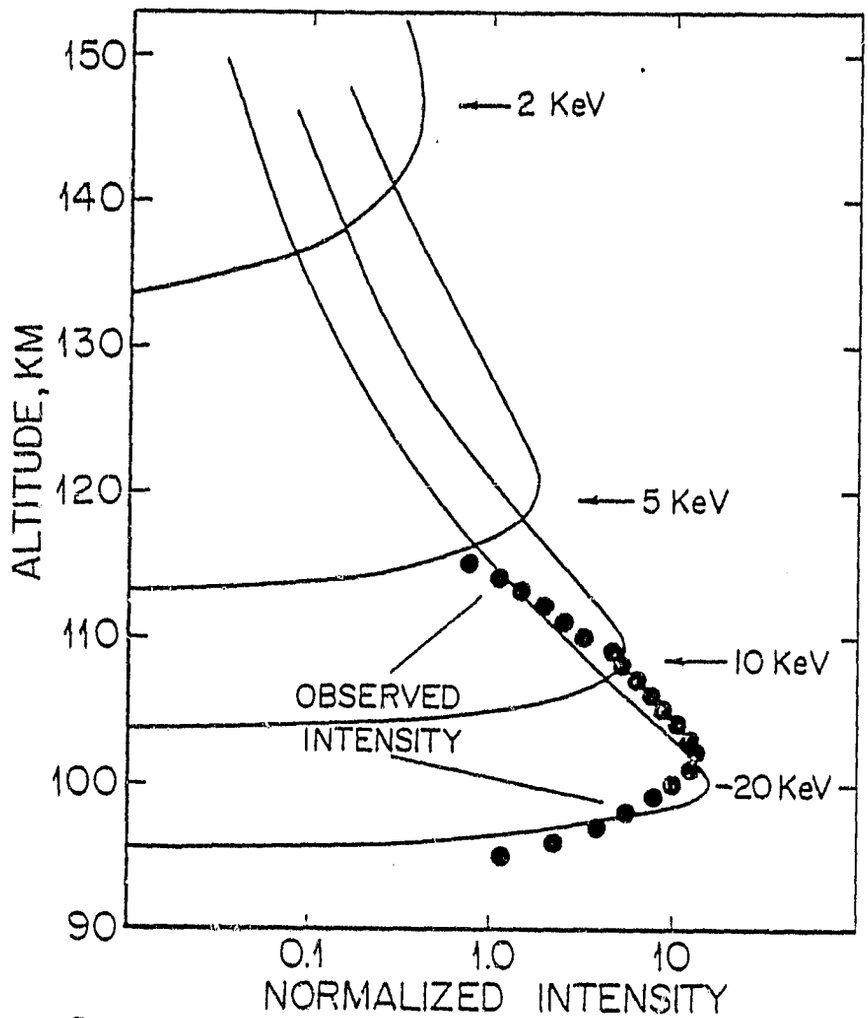


9

Profiles of energy deposition calculated for monoenergetic electron beams (solid lines) and a normalized plot of observed luminosity of the aurora resulting from pulse B44.